Asymptotic derivation of a higher-order one-dimensional model for tape springs

Arun Kumar, Basile Audoly, Claire Lestringant

Asymptotic derivation of a higher-order one-dimensional model for tape springs

Arun Kumar

Laboratoire de Mécanique des Solides
CNRS, Institut Polytechnique de Paris
91120 Palaiseau, France

Basile Audoly

Laboratoire de Mécanique des Solides
CNRS, Institut Polytechnique de Paris
91120 Palaiseau, France

Claire Lestringant

Institut Jean Le Rond d'Alembert,
Sorbonne Université, CNRS,
75005 Paris, France

We derive a one-dimensional model for tape springs. The derivation starts from nonlinear thin-shell theory and uses a dimension reduction technique that combines a centerline-based parameterization of the tape-spring mid-surface with the assumption that the strain varies slowly along the length of the tape spring. The one-dimensional model is effectively a higher-order rod model: at leading order, the strain energy depends on the extensional, bending and twisting strains and is consistent with classical results from the literature; the two following orders are novel and capture the dependence of the strain energy on the strain gradients. The cross-sectional displacements are solved as part of the dimension reduction process, making the one-dimensional model asymptotically exact. We expect that the model will accurately and efficiently capture the deformations and instabilities in tape springs, including those involving highly localized deformations.

1. Introduction

A tape spring (or "carpenter's tape") is a thin elastic strip endowed with a non-zero natural curvature c across its width. Its dimensions, namely length ℓ, width a, and thickness t, are very different from one another, with $\ell \gg a \gg t$. They can bend and twist easily, and exhibit a rich, severely nonlinear response. When subjected to opposite-sense bending, for instance, (the applied longitudinal curvature and the natural transverse curvature are in opposite directions), they undergo a snapping instability which leads to localization and to propagating instabilities involving the coexistence of two 'phases' having very different curvature [1]. On the other hand, equal-sense bending (the applied longitudinal curvature and the natural curvature are in the same direction) leads to a lateral-torsional buckling instability. These instabilities lead to large, repeatable, and sudden changes in their shape, which can be useful for packing and deployment applications such as deployable reflectors, telescopes and solar panels [2, 3, 4].

A standard approach for modeling tape springs involves using two-dimensional non-linear shell theory. This approach, although accurate, yields computationally costly simulations. Since tape springs are long and slender structures, a desirable alternative is to describe them using one-dimensional rod-like models, which are amenable to fast and robust numerical methods, such as Discrete elastic rods [5, 6] or numerical continuation using Auto07p [7].

An early work in this direction dates back to Wuest [8], who derived an analytical one-dimensional model capturing the deformation of a tape spring whose centerline is restricted to bend in a plane. Mansfield [9] later extended this approach to account for twisting. These models capture the up-down-up moment-curvature response that explains the snapping instabilities and the tendency for the deformation to localize [1]. They fail, however, to capture the localized solutions themselves, that entail large gradients of longitudinal curvature. Similar features are also encountered at interfaces in solid-solid phase transformations and arise from the non-convex character of the energy. A proper description of interfaces is known to require the energy to be regularized, by accounting not only for its dependence on the bending and twisting strains as in early models of Wuest and Mansfield, but also on the strain *gradient* [10, 11]. The goal of the present work is to derive a regularized energy for tape springs in a mathematically principled way.

In a recent series of papers [12, 13, 14, 11], a family of one-dimensional models for tape springs featuring strain-gradient regularization have been proposed. They have been applied to the analysis of localized solutions [11]. These models are based on kinematic ansatzes, *i.e.*, they work by parameterizing the deformation of the tape spring by a series of cross-sectional degrees of freedom, their accuracy being guaranteed only in the limit where infinitely many degrees of freedom are used: by design, they involve a trade-off between accuracy on the one hand, and efficiency and ease of use on the other hand. A related numerical approach has been developed by Carrera and others, see for instance [15, 16].

Our approach is different: we derive a one-dimensional energy for tape springs addressing the strain-gradient effect, using a dimension reduction method applicable to nonlinear elasticity problems and proposed recently by the authors [17]. The method is mathematically rigorous or, more specifically, *asymptotically exact*; it is not based on kinematic assumptions and does not introduce any cross-sectional degree of freedom. It has been applied to the analysis of propagating instabilities in nonlinear slender elastic structures such as cylindrical balloons [18] and elasto-capillary bars [19], where it has shown excellent accuracy. It has also been used to derive a one-dimensional model for extensible elastic ribbons recently [20] although the strain gradient has been ignored in this work—elastic ribbons are a particular case of tape springs corresponding to $c=0$.

Building up on this earlier work, we derive the following one-dimensional strain energy functional from a two-dimensional non-linear shell model,

$$\begin{aligned}\Phi^\star[\boldsymbol{\hbar}] \;=\; \int_0^\ell \Big(W^\star_{[0]}(\boldsymbol{\hbar}(S)) + \boldsymbol{A}(\boldsymbol{\hbar}(S))\cdot\boldsymbol{\hbar}'(S) + \frac{1}{2}\boldsymbol{\hbar}'(S)\cdot\boldsymbol{B}(\boldsymbol{\hbar}(S))\cdot\boldsymbol{\hbar}'(S)\Big)\,\mathrm{d}S \\ + \Big[\boldsymbol{C}(\boldsymbol{\hbar}(S))\cdot\boldsymbol{\hbar}'(S)\Big]_0^\ell + \cdots\end{aligned} \tag{1}$$

where the square bracket on the right-hand side denotes the variation of the enclosed quantity from the endpoint $S=0$ to the endpoint $S=\ell$ (boundary terms). The vector $\boldsymbol{\hbar}(S)=(\varepsilon(S),\kappa_1(S),\kappa_2(S),\kappa_3(S))$ collects the strains of the equivalent rod at a particular coordinate S along the centerline, namely the stretching strain $\varepsilon(S)$, the bending strains $\kappa_1(S)$ and $\kappa_2(S)$, and the twisting strain $\kappa_3(S)$. Note the dependence of the strain energy functional $\Phi^\star$ on the strain *gradient* $\boldsymbol{\hbar}'(S)=(\varepsilon'(S),\kappa_1'(S),\kappa_2'(S),\kappa_3'(S))$.

The strain energy functional $\Phi^\star$ is obtained by assuming that the strains vary slowly along the length,

$$\frac{\mathrm{d}^k\boldsymbol{\hbar}}{\mathrm{d}S}=\mathcal{O}(\gamma^k), \tag{2}$$

where $\gamma\ll 1$ is a small parameter, which is typically set by the aspect-ratio of the tape spring, $\gamma\sim a/\ell$. The right-hand side of (1) is derived by a systematic expansion in powers of γ, which could in principle be continued to an arbitrary order. The detailed expression of the leading order term $\int_0^\ell W^\star_{[0]}(\boldsymbol{\hbar}(S))\,\mathrm{d}S=\mathcal{O}(\ell\gamma^0)$ is given in (57) and it is consistent with previous work [9]. The subsequent orders capture the strain-gradient effect and are novel. The correction $\int_0^\ell \boldsymbol{A}(\boldsymbol{\hbar}(S))\cdot\boldsymbol{\hbar}'(S)\,\mathrm{d}S=\mathcal{O}(\ell\gamma^1)$ at order γ^1 involves a vector $\boldsymbol{A}$ whose expression is worked out in Subsection 5.2. A detailed recipe for calculating the matrix $\boldsymbol{B}$ and the vector $\boldsymbol{C}$ appearing in the next-order correction $\int_0^\ell \frac{1}{2}\boldsymbol{\hbar}'(S)\cdot\boldsymbol{B}(\boldsymbol{\hbar}(S))\cdot\boldsymbol{\hbar}'(S)\,\mathrm{d}S+\big[\boldsymbol{C}(\boldsymbol{\hbar}(S))\cdot\boldsymbol{\hbar}'(S)\big]_0^\ell=\mathcal{O}(\ell\gamma^2)$ is given in Subsection 5.3. The ellipsis in (1) stands for terms of order $\ell\gamma^3$ or higher that are ignored. Our main contribution is a method for computing the quantities $\boldsymbol{A}$, $\boldsymbol{B}$ and $\boldsymbol{C}$ for any value of their argument $\boldsymbol{\hbar}(S)$.

In addition to the fundamental assumption (2) of slow longitudinal variations, we make the following convenient scaling assumptions on the one-dimensional strain,

$$\varepsilon(S)=\mathcal{O}\Big(\frac{t^2}{a^2}\Big),\quad \kappa_1(S)=\mathcal{O}\Big(\frac{t}{a}\kappa^\star\Big),\quad \kappa_2(S)=\mathcal{O}(\kappa^\star),\quad \kappa_3(S)=\mathcal{O}(\kappa^\star),\quad c=\mathcal{O}(\kappa^\star), \tag{3}$$

where $\kappa^\star$ is a typical strain

$$\kappa^\star\sim t/a^2. \tag{4}$$

The scaling assumptions (3) arise naturally in the context of thin elastic ribbons [20]; they will allow us to use a moderate slope approximation—thereby simplifying the calculations—but could in principle be lifted.

This article is limited to the derivation of energy functional (1). We plan to apply the model to the tape spring problems in follow-up papers. The equilibrium equations required for obtaining the solutions can be derived variationally from (1) by adapting the approach presented in [21, Appendix A.1]: as shown in this work, the equilibrium equations of the one-dimensional model are governed by the standard Kirchhoff equations for nonlinear rods together with special constitutive relations which can be expressed in terms of the components of the elastic energy $W^\star_{[0]}$, $\boldsymbol{A}$ and $\boldsymbol{B}$.

2. Starting point: shell model

A tape spring is represented as a thin elastic shell made of an isotropic, linear elastic material with Young's modulus Y and Poisson's ratio ν. This section presents the thin shell model. It is based on geometric approximations consistent with the scaling assumptions (3–4).

2.1. Kinematic description

We first introduce a centerline-based parameterization of the tape spring. The centerline is an imaginary curve intended to provide a coarse-grained description of the tape spring. The centerline-based parameterization offers the advantage of using a set of variables that are suitable for dimension reduction [21, 20], namely macroscopic variables $\boldsymbol{\varkappa}$ characterizing the centerline (which are exposed in the one-dimensional energy $\Phi^\star[\boldsymbol{\varkappa}]$) and microscopic variables $\boldsymbol{y}$ capturing the detailed shape of the cross-sections (which we seek to eliminate).

The tape spring's midsurface is parameterized by Lagrangian coordinates $S\in[0,\ell]$ and $T\in[-a/2,a/2]$, which are the arc length coordinates measured in the undeformed configuration in the longitudinal and transverse directions, respectively. The width a is measured along the midsurface in the undeformed configuration, see Figure 1. A *cross-section* is the set of material points sharing the same coordinate S, as shown by the dashed curves in Figure 1.

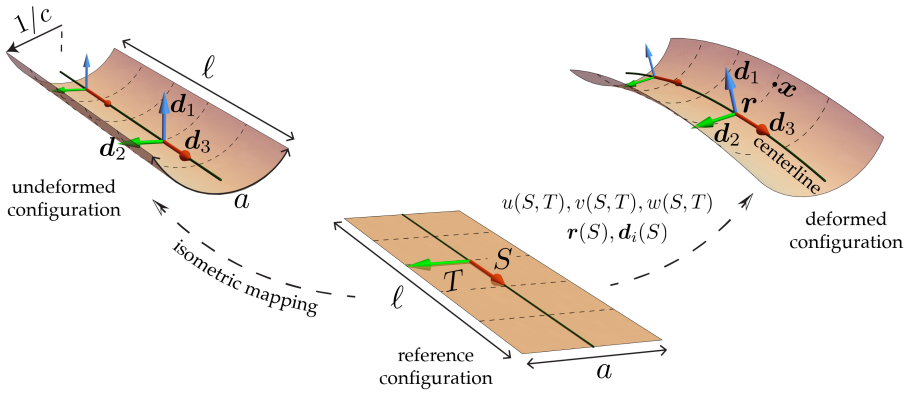

Figure 1. The *undeformed* midsurface (left) of the tape spring is a cylinder. The *reference* midsurface (center) is obtained by isometrically flattening out the undeformed midsurface into a rectangle $(S,T)\in[0,\ell]\times[-a/2,a/2]$. The *deformed* midsurface $\boldsymbol{x}(S,T)$ is parameterized by a centerline $\boldsymbol{r}(S)$, a frame of directors $\boldsymbol{d}_i(S)$ and microscopic displacements $u(S,T)$, $v(S,T)$ and $w(S,T)$. Cross-sections are shown by the dashed curves. The centerline $\boldsymbol{r}(S)$ passes through the centroid of every cross-section and therefore floats above the midsurface in the presence of transverse curvature.

The position $\boldsymbol{x}(S,T)$ of a point on the deformed midsurface of the tape spring is parameterized as

$$\boldsymbol{x}(S,T)=\boldsymbol{r}(S)+w(S,T)\,\boldsymbol{d}_1(S)+(T+u(S,T))\,\boldsymbol{d}_2(S)+v(S,T)\,\boldsymbol{d}_3(S). \tag{5}$$

where $\boldsymbol{r}(S)$ is the centerline, $(\boldsymbol{d}_1(S),\boldsymbol{d}_2(S),\boldsymbol{d}_3(S))$ is a frame of orthonormal vectors called *directors*,

$$\boldsymbol{d}_i(S)\cdot\boldsymbol{d}_j(S)=\delta_{ij}\qquad\forall S, \tag{6}$$

and $(u(S,T),v(S,T),w(S,T))$ are three scalar functions that capture the cross-sectional displacements measured in the directors frame; these displacements are measured with respect to the flat reference configuration. The symbol δ_{ij} in (6) denotes the Kronecker symbol, which equals to 1 if the indices are equal and to 0 otherwise. We will refer to (5) as the *centerline-based parameterization of the shell*; a similar parameterization has been used for prismatic three-dimensional solids in [22, 21] and for elastic plates in [20].

The centerline $\boldsymbol{r}$ is defined as the curve passing through the centroid $\boldsymbol{r}(S)$ of each one of cross-section labelled by S,

$$\boldsymbol{r}(S)=\langle\boldsymbol{x}(S,T)\rangle_T, \tag{7}$$

where the angular bracket denotes the average with respect to the transverse coordinate T,

$$\langle f(S,T)\rangle_T=\frac{1}{a}\int_{-a/2}^{+a/2}f(S,T)\,\mathrm{d}T. \tag{8}$$

Note that by (5) and (7) the cross-sectional displacements must average out to zero on every cross-section,

$$\langle w(S,T)\rangle_T=0,\quad\langle u(S,T)\rangle_T=0,\quad\langle v(S,T)\rangle_T=0\qquad\forall S. \tag{9}$$

The orthonormal frame of directors is prescribed by requiring that $\boldsymbol{d}_3(S)$ is the unit tangent to the centerline,

$$\boldsymbol{d}_3(S) = \frac{\boldsymbol{r}'(S)}{|\boldsymbol{r}'(S)|}, \tag{10}$$

and that $\boldsymbol{d}_1(S)$ is 'on average perpendicular' to the cross-section having coordinate S, as shown in Figure 1,

$$\langle T w(S,T)\rangle_T = 0 \qquad \forall S. \tag{11}$$

What we mean by 'on average perpendicular' is the following. We observe that the 'first moment' of the position $\langle T\,(\boldsymbol{x}(S,T) - \boldsymbol{r}(S))\rangle_T$ provides a notion of the average direction of the cross-section having coordinate S; by (5), the left-hand side of (11) is nothing but $\boldsymbol{d}_1(S)\cdot\langle T\,(\boldsymbol{x}(S,T) - \boldsymbol{r}(S))\rangle_T$.

The condition that the unit vector $\boldsymbol{d}_1(S)$ is perpendicular to both $\boldsymbol{d}_3(S)$ by (6), and to $\langle T\,(\boldsymbol{x}(S,T) - \boldsymbol{r}(S))\rangle_T$ fixes it up to a sign. This indeterminacy can be lifted, *e.g.*, by the convention that $\boldsymbol{d}_1(0)\cdot(\boldsymbol{x}_{,T}(0,0)\times\boldsymbol{x}_{,S}(0,0)) > 0$ and $\boldsymbol{d}_1(S)$ is continuous—the factor in parentheses in the dot product is the midsurface normal having the orientation naturally associated with the parameterization (S,T).

With directors $\boldsymbol{d}_1(S)$ and $\boldsymbol{d}_3(S)$ defined, the last director is obtained as $\boldsymbol{d}_2(S) = \boldsymbol{d}_3(S)\times\boldsymbol{d}_1(S)$, making the frame $(\boldsymbol{d}_1(S), \boldsymbol{d}_2(S), \boldsymbol{d}_3(S))$ positively oriented.

Remark 1. By contrast with a number of earlier papers on dimension reduction, we do not define the centerline $\boldsymbol{r}(S)$ as the material curve $\boldsymbol{x}(S,0)$. The centerline does not even lie on the deformed midsurface in general, see Figure 1.

Remark 2. The goal of dimension reduction is to eliminate the microscopic displacements $u(S,T)$, $v(S,T)$ and $w(S,T)$, and to deliver an equivalent rod model depending on just the centerline $\boldsymbol{r}(S)$ and the directors $\boldsymbol{d}_i(S)$. We will therefore call *equivalent rod* the collection of functions $\boldsymbol{r}$ (centerline) and $\boldsymbol{d}_i$ (directors frame) subjected to the kinematic constraints (6) and (10); this collection of a centerline curve and a compatible orthonormal frame is also known as a *framed centerline* in the literature [23].

Remark 3. The centerline-based parameterization of the midsurface in (5) is unique. Indeed, given a parameterization $\boldsymbol{x}(S,T)$ of the midsurface, the centerline $\boldsymbol{r}(S)$ can be obtained by (7) and the director $\boldsymbol{d}_3(S)$ by (10); the unit vector $\boldsymbol{d}_1(S)$ is uniquely defined, as discussed above. The displacements u, v and w are then found by taking the dot product of (5) with the directors. Note that the kinematic constraints (9) and (11) are required for the centerline-based parameterization to be unique: without (9) the centerline would no longer be tied to the actual position of the tape spring in space, and without (11) the directors $\boldsymbol{d}_1(S)$ and $\boldsymbol{d}_2(S)$ could freely rotate about $\boldsymbol{d}_3(S)$.

Remark 4. The only purpose of the directors frame $\boldsymbol{d}_i(S)$ is to keep track of twisting motions of the tape spring, whereby cross-sections rotate about the tangent $\boldsymbol{d}_3(S)$ while the centerline remains unchanged. This allows discriminating two configurations of the tape spring having the same centerline (same $\boldsymbol{r}$) but twisting differently about it (different $\boldsymbol{d}_1$ and $\boldsymbol{d}_2$).

Remark 5. The parameterization in (5) can capture an arbitrary configuration $\boldsymbol{x}(S,T)$ of the tape spring and entails no assumption on the solution of the elastic shell problem. In particular, Equations (6) or (10) do not assume that the tape spring is unshearable: thanks to the displacement $v(S,T)$ in (5), the cross-sections do not have to remain within a plane perpendicular to the centerline.

2.2. One-dimensional strain measures for the equivalent rod

The centerline displacement $\boldsymbol{r}(S)$ and directors $\boldsymbol{d}_i(S)$ come with standard strain measures in the theory of rods, which we proceed to introduce. The stretching strain $\varepsilon(S)$ is defined as

$$\boldsymbol{r}'(S) = (1+\varepsilon(S))\,\boldsymbol{d}_3(S), \tag{12}$$

where the alignment of $\boldsymbol{r}'(S)$ and $\boldsymbol{d}_3(S)$ is warranted by (10).

The rate of change of orthonormal director frame $(\boldsymbol{d}_1(S), \boldsymbol{d}_2(S), \boldsymbol{d}_3(S))$ with respect to the centerline coordinate S is measured by a Darboux vector $\boldsymbol{\kappa}(S) = \kappa_1(S)\,\boldsymbol{d}_1(S) + \kappa_2(S)\,\boldsymbol{d}_2(S) + \kappa_3(S)\,\boldsymbol{d}_3(S)$, also known as the rotation gradient, such that

$$\boldsymbol{d}_i'(S) = \boldsymbol{\kappa}(S)\times\boldsymbol{d}_i(S). \tag{13}$$

The component $\kappa_i(S) = \boldsymbol{\kappa}(S)\cdot\boldsymbol{d}_i(S)$ of the Darboux vector $\boldsymbol{\kappa}(S)$ furnish three additional strain measures. Both the twisting strain $\kappa_3(S)$ and the first bending strain $\kappa_1(S)$, which accounts for bending about $\boldsymbol{d}_1(S)$, are zero in the special case of the twistless, planar bending of a tape spring studied in the classical papers [8, 1]. The other bending strain $\kappa_2(S)$, which accounts for bending about $\boldsymbol{d}_2(S)$, is the quantity that localizes when the tape spring bends longitudinally [1]. We collect the strain measures for the equivalent rod in a vector $\boldsymbol{\mathcal{k}}(S) = (\varepsilon(S), \kappa_1(S), \kappa_2(S), \kappa_3(S))$, see (20) below.

2.3. Two-dimensional strain measures for the shell

By differentiating (5) with respect to either S or T, one obtains the tangents to the midsurface along the coordinate curves as

$$\begin{aligned}\boldsymbol{x}_{,T}(S,T) &= v_{,T}\boldsymbol{d}_3 + w_{,T}\boldsymbol{d}_1 + (1+u_{,T})\,\boldsymbol{d}_2.\\ \boldsymbol{x}_{,S}(S,T) &= (1+\varepsilon+v_{,S}-\kappa_2 w+\kappa_1(T+u))\,\boldsymbol{d}_3 + (w_{,S}-\kappa_3(T+u)+\kappa_2 v)\,\boldsymbol{d}_1 \ldots \\ &\qquad + (u_{,S}+\kappa_3 w-\kappa_1 v)\,\boldsymbol{d}_2\end{aligned} \tag{14}$$

Following classical shell theory, we introduce the membrane strain $\tilde{E}_{\alpha\beta} = (\boldsymbol{x}_{,\alpha}\cdot\boldsymbol{x}_{,\beta} - \delta_{\alpha\beta})/2$ capturing the stretching of the midsurface, and the bending strain $\tilde{B}_{\alpha\beta} = \boldsymbol{x}_{,\alpha\beta}\cdot\boldsymbol{n} - c\,\delta_{\alpha T}\delta_{\beta T}$, where $\boldsymbol{n} = (\boldsymbol{x}_{,T}\times\boldsymbol{x}_{,S})/|(\boldsymbol{x}_{,T}\times\boldsymbol{x}_{,S})|$ is the unit normal to the surface. In our notation, the Greek indices are restricted to in-plane directions, $\alpha,\beta\in\{S,T\}$.

Remark 6. The quantities $\tilde{E}_{\alpha\beta}$ and $\tilde{B}_{\alpha\beta}$ measure the changes in metric and curvature, respectively, from the *undeformed* to the *deformed* configurations:

- $\boldsymbol{x}_{,\alpha}\cdot\boldsymbol{x}_{,\beta}$ is the usual definition of the metric tensor on a parametric surface $\boldsymbol{x}(S,T)$. In the reference (rectangular) configuration, the vectors $(\boldsymbol{x}_{,S},\boldsymbol{x}_{,T})$ are of unit magnitude and orthogonal, yielding metric tensor equal to $\delta_{\alpha\beta}$. Since the undeformed configuration is connected to the reference configuration by an isometric mapping, its metric tensor is also $\delta_{\alpha\beta}$.
- the quantity $\boldsymbol{x}_{,\alpha\beta}\cdot\boldsymbol{n}$ is the classical curvature 2-form from differential geometry. In the cylindrical, undeformed configuration, this curvature 2-form is equal to $c\,\delta_{\alpha T}\delta_{\beta T}$ where c is the natural curvature of the tape spring in the transverse direction.

The scaling assumptions for the displacement and shell strains that are consistent with those for the one-dimensional strain in (3) and have been identified in previous work [20] as

$$u=\mathcal{O}\!\left(\frac{t^2}{a}\right),\quad v=\mathcal{O}\!\left(\frac{t^2}{a}\right),\quad w=\mathcal{O}(t),\quad \tilde{E}_{\alpha\beta}=\mathcal{O}\!\left(\frac{t^2}{a^2}\right),\quad \tilde{B}_{\alpha\beta}=\mathcal{O}(\kappa^\star),\quad \frac{\partial}{\partial S}\sim\frac{\partial}{\partial T}=\mathcal{O}\!\left(\frac{1}{a}\right). \tag{15}$$

In view of these scaling relations, the geometrically exact shell strains $\tilde{E}_{\alpha\beta}$ and $\tilde{B}_{\alpha\beta}$ can be simplified by dropping any term that is negligible compared to t^2/a^2 in $\tilde{E}_{\alpha\beta}$ (such as the contribution $\frac{1}{2}(\kappa_1 u\,\boldsymbol{d}_3)\cdot(\kappa_1 u\,\boldsymbol{d}_3)\sim\kappa_1^2u^2\sim(t^2/a^3)^2(t^2/a)^2\sim(t/a)^8\ll t^2/a^2$ in $\tilde{E}_{SS}$), and any term that is negligible compared to $\kappa^\star\sim t/a^2$ in $\tilde{B}_{\alpha\beta}$. The result is the approximate membrane strain

$$\begin{aligned}E_{SS}(S,T) &= \varepsilon(S)+T\kappa_1(S)-\kappa_2(S)\,w(S,T)+v_{,S}(S,T)+\frac{1}{2}(-T\kappa_3(S)+w_{,S}(S,T))^2\\ E_{TT}(S,T) &= u_{,T}(S,T)+\frac{1}{2}w_{,T}^2(S,T)\\ E_{ST}(S,T) &= \frac{1}{2}(\kappa_3(S)\,(w(S,T)-Tw_{,T}(S,T))+v_{,T}(S,T)+u_{,S}(S,T)+w_{,S}(S,T)w_{,T}(S,T))\end{aligned} \tag{16}$$

and the approximate bending strain

$$\begin{aligned}B_{SS}(S,T) &= \kappa_2(S)-\kappa_3'(S)\,T + w_{,SS}(S,T)\\ B_{TT}(S,T) &= w_{,TT}(S,T) - c\\ B_{ST}(S,T) &= -\kappa_3(S) + w_{,ST}(S,T).\end{aligned} \tag{17}$$

The approximate expressions $E_{\alpha\beta}$ and $B_{\alpha\beta}$ of the strains above are consistent with the scaling assumptions (3) and (15). The shell model that we use as the starting point for dimension reduction is based on them. A detailed derivation of Equations (16) and (17) can be found in [20, Appendix A.1], the only difference here being the $(-c)$ term in B_{TT} that accounts for the natural curvature of the tape spring.

Remark 7. The cylindrical, undeformed configuration is recovered by setting the one-dimensional strains to zero, $\varepsilon(S)=0$, $\kappa_1(S)=\kappa_2(S)=\kappa_3(S)=0$, and the microscopic displacement to $u(S,T)=-\frac{c^2}{6}T^3$, $v(S,T)=0$ and $w(S,T)=\frac{c}{2}(T^2-a^2/12)$. This solution indeed satisfies the kinematic constraints (9) and (11), and makes the shell strains zero, $E_{\alpha\beta}(S,T)=0$ and $B_{\alpha\beta}(S,T)=0$. Note that $E_{\alpha\beta}(S,T)=0$ is equivalent to $\tilde{E}_{\alpha\beta}(S,T)=0$ within our approximation scheme and it is in this sense that the mapping between the reference and undeformed configurations is isometric, see Figure 1. Relatedly, the polynomial solutions for u and v given above approximate the parametric equation for an arc of circle having curvature c by its arc length T in a way that is consistent with the scaling assumptions (3) and (15).

Remark 8. The strain approximation in (16–17) expresses that the midsurface rotates by a small amount relative to the directors, and is therefore akin to that underpinning the Föppl-von Kármán equations for plates. Indeed, the angle between the midsurface normal $\boldsymbol{x}_{,T}(S,T)\times\boldsymbol{x}_{,S}(S,T)$ and the *nearest* director $\boldsymbol{d}_1(S)$ can be shown to be of order $t/a\ll 1$ using the scaling assumptions (3) and (15). In undeformed configuration as well, the angle of deviation between the midsurface normal and the director $\boldsymbol{d}_1(S)$ is of order $c\,a$, *i.e.*, of order t/a, thanks to our scaling assumption $c=\mathcal{O}(\kappa^\star)$, see (3–4). Only the *relative* rotation of the midsurface with respect to the *nearest* directors is small: our shell model correctly accounts for finite rotations of the shell and its associated directors.

2.4. Constitutive relations and strain energy

According to shell theory, for a linearly elastic, isotropic material, the membrane stress $n_{\alpha\beta}$ and bending moment $m_{\alpha\beta}$ are given in terms of the membrane strain $E_{\alpha\beta}$ and bending strain $B_{\alpha\beta}$ by the following constitutive relation

$$\begin{pmatrix} n_{SS}\\ n_{TT}\\ n_{ST}\\ m_{SS}\\ m_{TT}\\ m_{ST}\end{pmatrix}=\boldsymbol{K}\begin{pmatrix} E_{SS}\\ E_{TT}\\ E_{ST}\\ B_{SS}\\ B_{TT}\\ B_{ST}\end{pmatrix},\qquad \text{where } \boldsymbol{K}=\begin{pmatrix} K\begin{pmatrix}1&\nu&0\\ \nu&1&0\\ 0&0&1-\nu\end{pmatrix} & \boldsymbol{0}\\ \boldsymbol{0} & D\begin{pmatrix}1&\nu&0\\ \nu&1&0\\ 0&0&1-\nu\end{pmatrix}\end{pmatrix}. \tag{18}$$

Here, $K=Yt/(1-\nu^2)$ and $D=Yt^3/(12\,(1-\nu^2))$ are the membrane and bending stiffnesses, respectively. The corresponding strain energy is quadratic with respect to the strain measures, and is given by

$$\Phi=\int_0^\ell\int_{-\frac{a}{2}}^{+\frac{a}{2}} W\,\mathrm{d}S\,\mathrm{d}T\quad\text{where } W=\frac{1}{2}\,(n_{\alpha\beta}\,E_{\alpha\beta}+m_{\alpha\beta}\,B_{\alpha\beta}). \tag{19}$$

In the equations above and throughout the article, we follow Einstein's implicit summation convention.

3. Strategy for dimension reduction

The centerline-based parameterization makes use of macroscopic and microscopic variables. Macroscopic variables characterize the centerline and directors: the associated strains (see Subsection 2.2) will be retained in the one-dimensional model. Microscopic variables capture the details of cross-sectional deformation. Their elimination from the energy (19) will furnish the equivalent one-dimensional model. A general recipe for carrying out this elimination is available from our previous work [17]. Before we can apply this recipe, we need to reformulate the shell model from Section 2 in a standard form called the *canonical form*, which provides the appropriate level of abstraction for carrying out dimension reduction. The canonical form of the shell model is obtained in Subsection 3.1. Subsection 3.2 presents the general strategy for the dimension reduction.

3.1. Casting the shell model in canonical form

The one-dimensional strains are collected in a vector $\boldsymbol{\mathfrak{h}}(S)$ as follows,

$$\boldsymbol{\mathfrak{h}}(S)=(\varepsilon(S),\kappa_1(S),\kappa_2(S),\kappa_3(S)). \tag{20}$$

The restrictions of the displacements to the cross-section with coordinate S are denoted as $u(S,\cdot)$, $v(S,\cdot)$ and $w(S,\cdot)$: each one of these objects is a function of the single variable T defined on $T\in[-a/2,+a/2]$. These three functions of T are collected in a vector we denote as $\boldsymbol{\mathfrak{y}}(S)$,

$$\boldsymbol{\mathfrak{y}}(S)=(u(S,\cdot),v(S,\cdot),w(S,\cdot)). \tag{21}$$

Remark 9. The macroscopic variables are collected in $\boldsymbol{\mathfrak{h}}(S)$, while the microscopic variables are collected in $\boldsymbol{\mathfrak{y}}(S)$. Together, functions $\boldsymbol{\mathfrak{h}}$ and $\boldsymbol{\mathfrak{y}}$ specify the tape spring configuration up to a rigid-body motion, and are the arguments of the strain energy of the shell model, see (27). By itself, the function $\boldsymbol{\mathfrak{h}}$ characterizes the equivalent rod (or *framed centerline*) up to a rigid-body motion, and it is the sole argument of the one-dimensional strain energy functional $\Phi^\star$ in (1).

Given a particular value of S, we denote as $\boldsymbol{y} = \boldsymbol{\mathcal{y}}(S)$ the microscopic variables at the corresponding cross-section. In view of (21), the components $\boldsymbol{y}$, which we denote as $\boldsymbol{y} = (y_u, y_v, y_w)$, are the restrictions $(u(S,\cdot), v(S,\cdot), w(S,\cdot))$ of the displacement. Therefore, we have $y_u(T) = u(S,T)$, $y_v(T) = v(S,T)$ and $y_w(T) = w(S,T)$. We will also denote by $\boldsymbol{y}^\dagger = (y_u^\dagger, y_v^\dagger, y_w^\dagger) = \boldsymbol{\mathcal{y}}'(S)$ the restrictions of the *longitudinal* gradients of the displacement, such as $y_u^\dagger(T) = \partial_S u(S,T)$, and by $\boldsymbol{y}^\ddagger = (y_u^\ddagger, y_v^\ddagger, y_w^\ddagger) = \boldsymbol{\mathcal{y}}''(S)$ the restrictions of the second longitudinal gradients of displacement to the cross-section at S, such as $y_u^\ddagger(T) = \partial_{SS} u(S,T)$. Note that the *transverse* gradient of a cross-sectional displacement can be directly obtained by differentiating the restrictions, as in $\partial_T u(S,T) = \partial_T y_u(T)$.

Similarly, we will denote by $\boldsymbol{h} = (\varepsilon, \kappa_1, \kappa_2, \kappa_3) = \boldsymbol{\mathcal{h}}(S) \in \mathbb{R}^4$ the values of the one-dimensional strain at a particular cross-section at S, by $\boldsymbol{h}^\dagger = (\varepsilon^\dagger, \kappa_1^\dagger, \kappa_2^\dagger, \kappa_3^\dagger) = \boldsymbol{\mathcal{h}}'(S) \in \mathbb{R}^4$ the values of the strain gradient, and by $\boldsymbol{h}^\ddagger = (\varepsilon^\ddagger, \kappa_1^\ddagger, \kappa_2^\ddagger, \kappa_3^\ddagger) = \boldsymbol{\mathcal{h}}''(S) \in \mathbb{R}^4$ the values of the second gradient of strain at S, such that for instance $\varepsilon^\ddagger = \varepsilon''(S)$.

Remark 10. We use calligraphic symbols to emphasize that a quantity is a *function*, such as $\boldsymbol{\mathcal{h}}$ or $\boldsymbol{\mathcal{y}}$, and distinguish from its *value* using roman symbols, such as $\boldsymbol{h} = \boldsymbol{\mathcal{h}}(S)$ or $\boldsymbol{y} = \boldsymbol{\mathcal{y}}(S)$. Mathematically, $\boldsymbol{h} \in \mathbb{R}^4$ is a vector while $\boldsymbol{\mathcal{h}}$ is a function of S whose *values* are vectors, and $\boldsymbol{y}$ is a vector made up of three functions of T while $\boldsymbol{\mathcal{y}}$ is a function of S whose values are vectors made up of three functions of T. A similar notation is also used later for the membrane and bending strains, see (26), and for the strain energy per unit length, which we write as $W = \mathcal{W}(\boldsymbol{E})$.

To express the kinematic constraints (9) and (11) in compact form, we define a functional $\boldsymbol{\mathcal{Q}}$ taking a vector $\boldsymbol{y} = (y_u, y_v, y_w)$ of cross-sectional functions $y_u(T)$, $y_v(T)$ and $y_w(T)$ as arguments as follows,

$$\boldsymbol{\mathcal{Q}}\boldsymbol{y} = \big(\langle y_u(T)\rangle_T, \langle y_v(T)\rangle_T, \langle y_w(T)\rangle_T, \langle T y_w(T)\rangle_T\big). \tag{22}$$

The kinematic constraints (9) and (11) can then be rewritten as

$$\boldsymbol{\mathcal{Q}}\boldsymbol{\mathcal{y}}(S) = \boldsymbol{0} \qquad \forall S. \tag{23}$$

At a particular point on the midsurface with coordinates (S,T), the membrane and bending strains from the shell model are collected into a vector denoted by $\boldsymbol{E}$ with the following ordering convention,

$$\boldsymbol{E} = \big(E_{SS}(S,T), E_{TT}(S,T), E_{ST}(S,T), B_{SS}(S,T), B_{TT}(S,T), B_{ST}(S,T)\big). \tag{24}$$

Equations (16) and (17) yielding the strain measures of the shell model can then be cast in the form

$$\boldsymbol{E} = \boldsymbol{\mathcal{E}}(T; \boldsymbol{\mathcal{h}}(S), \boldsymbol{\mathcal{h}}'(S); \boldsymbol{\mathcal{y}}(S), \boldsymbol{\mathcal{y}}'(S), \boldsymbol{\mathcal{y}}''(S)) \tag{25}$$

where $\boldsymbol{\mathcal{E}}$ is the function

$$\boldsymbol{\mathcal{E}}(T; \boldsymbol{h}, \boldsymbol{h}^\dagger; \boldsymbol{y}, \boldsymbol{y}^\dagger, \boldsymbol{y}^\ddagger) = \left(\begin{array}{c} \varepsilon + T\kappa_1 - \kappa_2\, y_w(T) + y_v^\dagger(T) + \frac{1}{2}\,(-T\kappa_3 + y_w^\dagger(T))^2 \\ \partial_T y_u(T) + \frac{1}{2}\,(\partial_T y_w(T))^2 \\ \hline \frac{1}{2}\,(\kappa_3\,(y_w(T) - T\partial_T y_w(T)) + \partial_T y_v(T) + y_u^\dagger(T) + y_w^\dagger(T)\,\partial_T y_w(T)) \\ \hline \kappa_2 - T\kappa_3^\dagger + y_w^\ddagger(T) \\ \partial_{TT} y_w(T) - c \\ -\kappa_3 + \partial_T y_w^\dagger(T) \end{array}\right) \tag{26}$$

The optional horizontal bar separates the three membrane strain components of $\boldsymbol{E}$ with its three bending strain components.

Remark 11. The quantities in the right-hand side of (26) are related to those passed in arguments of the left-hand side through our notation $\boldsymbol{h} = (\varepsilon, \kappa_1, \kappa_2, \kappa_3)$, $\boldsymbol{h}^\dagger = (\varepsilon^\dagger, \kappa_1^\dagger, \kappa_2^\dagger, \kappa_3^\dagger)$, $\boldsymbol{y} = (y_u, y_v, y_w)$, etc.

Remark 12. One can check the equivalence of (16) and (17) on the one hand with (25) and (26) on the other hand as follows. Equation (25) is an equality between two vectors having six components. Let us consider the fourth component, for instance, which is $B_{SS}(S,T) = \kappa_2 + y_w^\ddagger(T) - T\kappa_3^\dagger$ by (24). Identifying the arguments $\boldsymbol{h} = (\varepsilon_1, \kappa_1, \dots)$, $\boldsymbol{h}^\dagger = (\varepsilon_1^\dagger, \kappa_1^\dagger, \dots)$, $\boldsymbol{y} = (y_u, y_v, y_w)$, etc. of $\boldsymbol{\mathcal{E}}$ in (26) with the values $\boldsymbol{\mathcal{h}}(S) = (\varepsilon_1(S), \kappa_1(S), \dots)$, $\boldsymbol{\mathcal{h}}'(S) = (\varepsilon_1'(S), \kappa_1'(S), \dots)$, $\boldsymbol{\mathcal{y}}(S) = (u(S,\cdot), v(S,\cdot), w(S,\cdot))$ passed in argument in (25), we get $B_{SS}(S,T) = \kappa_2(S) + \partial_{SS} w(T) - T\kappa_3'(S)$, which is nothing but the first component in (17).

Finally, the strain energy in (19) can be rewritten as

$$\Phi[\boldsymbol{\mathcal{R}},\boldsymbol{\mathcal{Y}}]=\int_0^\ell\int_{-\frac{a}{2}}^{+\frac{a}{2}}\mathcal{W}(\boldsymbol{\mathcal{E}}(T;\boldsymbol{\mathcal{R}}(S),\boldsymbol{\mathcal{R}}'(S);\boldsymbol{\mathcal{Y}}(S),\boldsymbol{\mathcal{Y}}'(S),\boldsymbol{\mathcal{Y}}''(S)))\,\mathrm{d}S\,\mathrm{d}T \tag{27}$$

where the strain energy density $W=\mathcal{W}(\boldsymbol{E})$ is given in terms of the shell strain measures $\boldsymbol{E}$ as

$$\mathcal{W}(\boldsymbol{E})=\frac{1}{2}\boldsymbol{\Sigma}(\boldsymbol{E})*\boldsymbol{E}, \tag{28}$$

and $\boldsymbol{\Sigma}(\boldsymbol{E})=(n_{SS},n_{TT},n_{ST},m_{SS},m_{TT},m_{ST})$ denotes the internal (membrane and bending) stresses, given by the constitutive relation (18) as

$$\boldsymbol{\Sigma}(\boldsymbol{E})=\boldsymbol{K}\,\boldsymbol{E}. \tag{29}$$

In (28), the $*$ product represents the contraction of the pair of tangent indices α and β appearing in the energy density in (19),

$$\boldsymbol{\Sigma}*\boldsymbol{E}=\boldsymbol{\Sigma}\cdot\mathrm{diag}(1,1,2,1,1,2)\cdot\boldsymbol{E}, \tag{30}$$

where diag stands for a diagonal matrix. The consistency with the contraction of indices can be verified as follows: $E_{\alpha\beta}n_{\alpha\beta}+B_{\alpha\beta}m_{\alpha\beta}=E_{SS}n_{SS}+E_{TT}n_{TT}+E_{ST}n_{ST}+E_{TS}n_{TS}+B_{SS}m_{SS}+B_{TT}m_{TT}+B_{ST}m_{ST}+B_{TS}m_{TS}=E_{SS}n_{SS}+E_{TT}n_{TT}+2\,E_{ST}n_{ST}+B_{SS}m_{SS}+B_{TT}m_{TT}+2\,B_{ST}m_{ST}=\boldsymbol{\Sigma}\cdot\mathrm{diag}(1,1,2,1,1,2)\cdot\boldsymbol{E}$.

For later reference, we note that the gradient of $\mathcal{W}$ in the direction $\hat{\boldsymbol{E}}$ is given as

$$\mathrm{D}_{\boldsymbol{E}}\mathcal{W}(\boldsymbol{E};\hat{\boldsymbol{E}})=\boldsymbol{\Sigma}(\boldsymbol{E})*\hat{\boldsymbol{E}}=(\boldsymbol{K}\,\boldsymbol{E})*\hat{\boldsymbol{E}}. \tag{31}$$

In Equations (23), (26) and (27), respectively, we have obtained expressions for the kinematic constraints, the microscopic strain and the strain energy functional that conform with the canonical form proposed in our previous work.

3.2. Dimension reduction

The first key ingredient in the model derivation is the *elimination of the microscopic displacement*. For a prescribed $\boldsymbol{\mathcal{R}}$, we eliminate $\boldsymbol{\mathcal{Y}}$ by assuming that the optimal $\boldsymbol{\mathcal{Y}}$ is the stationary point of the energy among all $\boldsymbol{\mathcal{Y}}$'s satisfying the constraint (23). The problem is to find $\boldsymbol{\mathcal{Y}}$ and $\boldsymbol{\mathcal{F}}$ that are the solutions of

$$\begin{aligned}\mathrm{D}_{\boldsymbol{\mathcal{Y}}}\Phi[\boldsymbol{\mathcal{R}},\boldsymbol{\mathcal{Y}};\hat{\boldsymbol{\mathcal{Y}}}]-\int_0^\ell\boldsymbol{\mathcal{F}}(S)\cdot\boldsymbol{\mathcal{Q}}\hat{\boldsymbol{\mathcal{Y}}}(S)\,\mathrm{d}S &= 0 \qquad (\forall\hat{\boldsymbol{\mathcal{Y}}}(S))\\ \boldsymbol{\mathcal{Q}}\boldsymbol{\mathcal{Y}}(S) &= \boldsymbol{0} \qquad \forall S\end{aligned} \tag{32}$$

where $\boldsymbol{\mathcal{F}}(S)=(\mathcal{F}_S(S),\mathcal{F}_T(S),\mathcal{F}_\mathrm{n}(S),\mathcal{F}_\mathrm{t}(S))$ is the Lagrange multiplier associated with the constraint $\boldsymbol{\mathcal{Q}}\boldsymbol{\mathcal{Y}}(S)=0$ in (23). Using the same typographical convention as in Remark 10, the value of the Lagrange multiplier at S will be denoted as $\boldsymbol{f}=(f_S,f_T,f_\mathrm{n},f_\mathrm{t})=\boldsymbol{\mathcal{F}}(S)$.

The solution of (32) is supposed to be unique, and is denoted as $\boldsymbol{\mathcal{Y}}=\boldsymbol{\mathcal{Y}}^\star[\boldsymbol{\mathcal{R}}]$ and $\boldsymbol{\mathcal{F}}=\boldsymbol{\mathcal{F}}^\star[\boldsymbol{\mathcal{R}}]$. This elimination of the microscopic displacement $\boldsymbol{\mathcal{Y}}$ yields an energy functional depending on the macroscopic strain only,

$$\Phi^\star[\boldsymbol{\mathcal{R}}]=\Phi[\boldsymbol{\mathcal{R}},\boldsymbol{\mathcal{Y}}^\star[\boldsymbol{\mathcal{R}}]]. \tag{33}$$

Obtaining the strain energy functional $\Phi^\star[\boldsymbol{\mathcal{R}}]$ is the ultimate goal of the dimension reduction. Unfortunately, the variational problem (32) entails solving nonlinear partial differential equations on the midsurface, and is intractable in general, so that $\Phi^\star[\boldsymbol{\mathcal{R}}]$ is not available in closed form.

The second key ingredient in the model derivation is to assume *slow variations in the longitudinal direction*: we complement the fundamental assumption (2) by a scaling assumption on the microscopic displacement,

$$\frac{\mathrm{d}^k\boldsymbol{\mathcal{R}}}{\mathrm{d}S^k}=\mathcal{O}(\gamma^k)\quad\text{and}\quad\frac{\mathrm{d}^k\boldsymbol{\mathcal{Y}}}{\mathrm{d}S^k}=\mathcal{O}(\gamma^k),$$

where γ is a small parameter related to the aspect-ratio, typically $\gamma\sim a/\ell$.

Next, we seek the optimum $\boldsymbol{\mathcal{Y}}^\star[\boldsymbol{\mathcal{R}}]$ of the variational problem (32) as a series expansion in powers of γ,

$$\boldsymbol{\mathcal{Y}}^\star[\boldsymbol{\mathcal{R}}]=\boldsymbol{\mathcal{Y}}^\star_{[0]}[\boldsymbol{\mathcal{R}}]+\boldsymbol{\mathcal{Y}}^\star_{[1]}[\boldsymbol{\mathcal{R}}]+\boldsymbol{\mathcal{Y}}^\star_{[2]}[\boldsymbol{\mathcal{R}}]+\cdots \tag{34}$$

where the $\boldsymbol{\mathcal{Y}}^\star_{[k]}[\boldsymbol{\mathcal{R}}]$'s denote the solutions obtained order by order in γ, *i.e.*, $\boldsymbol{\mathcal{Y}}^\star_{[k]}[\boldsymbol{\mathcal{R}}]=\mathcal{O}(\gamma^k)$. Inserting this order-by-order solution for the microscopic displacement into (33), one gets an expansion of the strain energy in the form

$$\Phi^\star[\boldsymbol{\mathcal{R}}]=\Phi^\star_{[0]}[\boldsymbol{\mathcal{R}}]+\Phi^\star_{[1]}[\boldsymbol{\mathcal{R}}]+\Phi^\star_{[2]}[\boldsymbol{\mathcal{R}}]+\cdots, \tag{35}$$

where $\Phi^\star_{[k]}[\boldsymbol{\hbar}] = \mathcal{O}(\gamma^k)$ is the contribution of order γ^k. The next two sections aim at obtaining the contributions $\Phi^\star_{[0]}[\boldsymbol{\hbar}]$, $\Phi^\star_{[1]}[\boldsymbol{\hbar}]$ and $\Phi^\star_{[2]}[\boldsymbol{\hbar}]$.

4. Leading-order solution

In this section, we derive the leading-order solution explicitly. The outcome is the strain energy functional $\Phi^\star_{[0]}[\boldsymbol{\hbar}]$ of the equivalent rod model at leading order, which is known from the previous work of Mansfield [9], as well as quantities such as the internal stress $\boldsymbol{\Sigma}^\star_{[0]}(T;\boldsymbol{h})$ that will be required to compute the gradient effect in Section 5, see $(55)_2$.

4.1. Plan for the leading order

At order γ^0, we can ignore all the *longitudinal* gradients in (27), which yields $\Phi[\boldsymbol{\hbar},\boldsymbol{y}] \approx \Phi_{[0]}[\boldsymbol{\hbar},\boldsymbol{y}] + \mathcal{O}(\gamma)$ where $\Phi_{[0]}[\boldsymbol{\hbar},\boldsymbol{y}] = \int_0^\ell \int_{-\frac{a}{2}}^{+\frac{a}{2}} \mathcal{W}(\boldsymbol{\mathcal{E}}_{[0]}(T;\boldsymbol{\hbar}(S);\boldsymbol{y}(S)))\,\mathrm{d}T\,\mathrm{d}S$ with

$$\boldsymbol{\mathcal{E}}_{[0]}(T;\boldsymbol{h};\boldsymbol{y}) = \boldsymbol{\mathcal{E}}(T;\boldsymbol{h},\boldsymbol{0};\boldsymbol{y},\boldsymbol{0},\boldsymbol{0}). \tag{36}$$

Inserting the expression of $\Phi_{[0]}$ into (32), applying the chain rule to differentiate $\mathcal{W}(\boldsymbol{\mathcal{E}}_{[0]}(T;\boldsymbol{\hbar}(S);\boldsymbol{y}(S)))$ with respect to $\boldsymbol{y}$, and by identifying the gradient $\mathrm{D}_{\boldsymbol{E}}\mathcal{W}$ from (31), we get

$$\int_0^\ell \left(\int_{-\frac{a}{2}}^{+\frac{a}{2}} (\boldsymbol{K}\boldsymbol{\mathcal{E}}_{[0]}(T;\boldsymbol{\hbar}(S);\boldsymbol{y}(S))) * \mathrm{D}_{\boldsymbol{y}}\boldsymbol{\mathcal{E}}_{[0]}(T;\boldsymbol{\hbar}(S);\boldsymbol{y}(S);\hat{\boldsymbol{y}}(S))\,\mathrm{d}T - \boldsymbol{\ell}(S)\cdot\boldsymbol{\mathcal{Q}}\hat{\boldsymbol{y}}(S) \right) \mathrm{d}S = 0. \tag{37}$$

for any perturbation $\hat{\boldsymbol{y}}$, together with the kinematic condition $\boldsymbol{\mathcal{Q}}\boldsymbol{y}(S) = \boldsymbol{0}$ for all S. In the variational problem above, the trial function $\hat{\boldsymbol{y}}(S)$ does not appear in derivatives with respect to S, implying that the solution $\boldsymbol{y}(S)$ can be found by solving the following *local* problem on a cross-section: given a macroscopic strain *value* $\boldsymbol{h}$, find the solution $(\boldsymbol{y},\boldsymbol{f})$ satisfying

$$\begin{aligned} \int_{-\frac{a}{2}}^{+\frac{a}{2}} (\boldsymbol{K}\boldsymbol{\mathcal{E}}_{[0]}(T;\boldsymbol{h},\boldsymbol{y})) * \mathrm{D}_{\boldsymbol{y}}\boldsymbol{\mathcal{E}}_{[0]}(T;\boldsymbol{h},\boldsymbol{y};\hat{\boldsymbol{y}})\,\mathrm{d}T - \boldsymbol{f}\cdot\boldsymbol{\mathcal{Q}}\hat{\boldsymbol{y}} = 0 \quad , \quad \forall \hat{\boldsymbol{y}} \\ \boldsymbol{\mathcal{Q}}\boldsymbol{y} = \boldsymbol{0}. \end{aligned} \tag{38}$$

As we will confirm later, the solution $\boldsymbol{y}$ to the cross-sectional problem (38) is unique. It depends on $\boldsymbol{h}$ only, and will be denoted as

$$\boldsymbol{y} = \boldsymbol{Y}^{\boldsymbol{h}}. \tag{39}$$

The quantity $\boldsymbol{Y}^{\boldsymbol{h}}$ will be referred to as the *catalog* of leading-order solutions. It can be calculated analytically in favorable circumstances, or numerically.

Remark 13. The notation introduced in Remark 10 plays a key role here. The input $\boldsymbol{h} = (\varepsilon,\kappa_1,\kappa_2,\kappa_3)$ of the cross-sectional problem (38) are four real numbers (which are *local* values of the one-dimensional strain), and the output is three functions $\boldsymbol{y} = (y_u, y_v, y_w)$ of the single variable T, capturing how the cross-section deforms in response to $\boldsymbol{h}$.

Equation (38) showed that the leading-order solution $\boldsymbol{y}(S) = \boldsymbol{y}^\star_{[0]}[\boldsymbol{\hbar}]$ to the (global) problem (37) is obtained simply by looking up the catalog $\boldsymbol{Y}^{\boldsymbol{h}}$ with the local value $\boldsymbol{\hbar}(S)$ of the strain,

$$\boldsymbol{y}^\star_{[0]}[\boldsymbol{\hbar}](S) = \boldsymbol{Y}^{\boldsymbol{\hbar}(S)}. \tag{40}$$

The catalog $\boldsymbol{Y}^{\boldsymbol{h}}$ of solutions to the local problem (38) on a cross-section is therefore the only ingredient needed to compute the energy at leading order. Specifically, it is used to define the leading-order predictions for the strain $\boldsymbol{\mathcal{E}}^\star_{[0]}$, the stress $\boldsymbol{\Sigma}^\star_{[0]}$, and the strain energy density $W^\star_{[0]}$ as

$$\begin{aligned} \boldsymbol{\mathcal{E}}^\star_{[0]}(T;\boldsymbol{h}) &= \boldsymbol{\mathcal{E}}_{[0]}(T;\boldsymbol{h};\boldsymbol{Y}^{\boldsymbol{h}}) \\ \boldsymbol{\Sigma}^\star_{[0]}(T;\boldsymbol{h}) &= \boldsymbol{K}\,\boldsymbol{\mathcal{E}}^\star_{[0]}(T;\boldsymbol{h}) \\ W^\star_{[0]}(\boldsymbol{h}) &= \int_{-\frac{a}{2}}^{+\frac{a}{2}} \mathcal{W}(\boldsymbol{\mathcal{E}}^\star_{[0]}(T;\boldsymbol{h}))\,\mathrm{d}T \end{aligned} \tag{41}$$

The leading-order contribution to the energy hence writes

$$\Phi^\star_{[0]}[\boldsymbol{\hbar}] = \int_0^\ell W^\star_{[0]}(\boldsymbol{\hbar}(S))\,\mathrm{d}S, \tag{42}$$

in accord with (1).

We proceed to carry out this plan in the next subsection. An analytical expression of $W^\star_{[0]}(\boldsymbol{h})$ is obtained in Equation (57).

Remark 14. The variational problem (38) at leading order can also be obtained by focusing on homogeneous solutions, *i.e.*, on configurations of the tape spring such that the one-dimensional strains ε, κ_1, κ_2 and κ_3 are independent of S. Indeed, the strain gradients that have been neglected at leading order, see (36), are exactly zero for these homogeneous solutions. For these homogeneous solutions, the centerline is a circular helix, an arc of a circle or a straight line, and the microscopic displacements are independent of S.

4.2. Leading-order displacement

The solution procedure at leading order is similar to that described in [20, Appendix A] for strips (case $c=0$). The leading-order expression (36) of the strain $\boldsymbol{\mathcal{E}}_{[0]}(T;\boldsymbol{h};\boldsymbol{y})=(E^{[0]}_{SS},E^{[0]}_{TT},E^{[0]}_{ST},B^{[0]}_{SS},B^{[0]}_{TT},B^{[0]}_{ST})$ is obtained by discarding the gradient terms in (16) and (17),

$$\begin{aligned} E^{[0]}_{SS} &= \varepsilon+T\kappa_1-\kappa_2\,y_w+\frac{1}{2}(T\kappa_3)^2 & B^{[0]}_{SS} &= \kappa_2\\ E^{[0]}_{TT} &= \partial_T y_u+\frac{1}{2}(\partial_T y_w)^2 & B^{[0]}_{TT} &= \partial_{TT}y_w-c\\ E^{[0]}_{ST} &= \frac{1}{2}\{\kappa_3(y_w-T\partial_T y_w)+\partial_T y_v\} & B^{[0]}_{ST} &= -\kappa_3 \end{aligned} \tag{43}$$

The stress $\boldsymbol{\Sigma}_{[0]}=(n^{[0]}_{SS},n^{[0]}_{TT},n^{[0]}_{ST},m^{[0]}_{SS},m^{[0]}_{TT},m^{[0]}_{ST})$ is calculated using the constitutive law $\boldsymbol{\Sigma}_{[0]}(T;\boldsymbol{h};\boldsymbol{y})=\boldsymbol{K}\boldsymbol{\mathcal{E}}_{[0]}(T;\boldsymbol{h};\boldsymbol{y})$, *i.e.*, $n^{[0]}_{SS}=K\,(E^{[0]}_{SS}+\nu E^{[0]}_{TT})$, etc. Inserting these stress and strain expressions into (38), we obtain the following variational problem: given $\boldsymbol{h}=(\varepsilon,\kappa_1,\kappa_2,\kappa_3)$, find $\boldsymbol{y}$ and $\boldsymbol{f}$ such that $\boldsymbol{\mathcal{Q}}\boldsymbol{y}=\boldsymbol{0}$ and, for any set of functions $(\hat{y}_u,\hat{y}_v,\hat{y}_w)$ of the single variable T,

$$\begin{aligned} -\int_{-\frac{a}{2}}^{+\frac{a}{2}}\Bigg\{ & f_S\,\hat{y}_v(T)-n^{[0]}_{ST}(T)\,\partial_T\hat{y}_v(T)+f_T\,\hat{y}_u(T)-n^{[0]}_{TT}(T)\,\partial_T\hat{y}_u(T)\\ & +\begin{pmatrix}\kappa_2\,n^{[0]}_{SS}(T)-\kappa_3\,n^{[0]}_{ST}(T)\\ +f_{\mathrm{n}}+f_{\mathrm{t}}\,T\end{pmatrix}\hat{y}_w(T)-\begin{pmatrix}n^{[0]}_{TT}(T)\,\partial_T y_w(T)\\ -\kappa_3\,T\,n^{[0]}_{ST}(T)\end{pmatrix}\partial_T\hat{y}_w(T)-m^{[0]}_{TT}(T)\,\partial_{TT}\hat{y}_w(T)\Bigg\}\,\mathrm{d}T \;=\; 0. \end{aligned}$$

For brevity, the dependence of the stress on $\boldsymbol{h}$ and $\boldsymbol{y}$ will be implicit in this subsection, *i.e.*, we use the short forms $\boldsymbol{\Sigma}_{[0]}(T)$, $n^{[0]}_{SS}(T)$, etc., for $\boldsymbol{\Sigma}_{[0]}(T;\boldsymbol{h};\boldsymbol{y})$, $n^{[0]}_{SS}(T;\boldsymbol{h},\boldsymbol{y})$, etc.

Using integration by parts twice, we get the equilibrium equations in strong form as

$$\begin{aligned} \partial_T n^{[0]}_{ST}(T)+f_S &= 0, & \partial_T q_T{}^{[0]}(T)+\kappa_2\,n^{[0]}_{SS}(T)-\kappa_3\,n^{[0]}_{ST}(T)+f_{\mathrm{n}}+f_{\mathrm{t}}\,T &= 0,\\ \partial_T n^{[0]}_{TT}(T)+f_T &= 0, & \boldsymbol{\mathcal{Q}}(y_u,y_v,y_w) &= 0. \end{aligned} \tag{44}$$

as well the natural boundary conditions on the lateral edges of the tape spring,

$$\begin{aligned} n^{[0]}_{TT}(\pm a/2) &= 0 & q^{[0]}_T(\pm a/2) &= 0\\ n^{[0]}_{ST}(\pm a/2) &= 0 & m^{[0]}_{TT}(\pm a/2) &= 0. \end{aligned} \tag{45}$$

where $q^{[0]}_T(T)=-\kappa_3\,T\,n^{[0]}_{ST}(T)-\partial_T m^{[0]}_{TT}(T)+n^{[0]}_{TT}(T)\,\partial_T y_w(T)$ is the shear force. Integrating the two equations in the first column of (44) and using boundary conditions in the first column of (45), we conclude that $f_S=f_T=0$ and that two in-plane stresses vanish identically, $n^{[0]}_{TT}=0$ and $n^{[0]}_{ST}=0$. Using (18) and (43), we find that y_u and y_v can be eliminated in favor of y_w by

$$\partial_T y_u=-\nu\left(\varepsilon+\kappa_1\,T+\frac{\kappa_3^2}{2}\,T^2-\kappa_2\,y_w\right)-\frac{(\partial_T y_w)^2}{2},\qquad \partial_T y_v=\kappa_3\,(-y_w+T\partial_T y_w). \tag{46}$$

There remains to solve for y_w. The procedure is identical to that described in [20, Appendix A] and can be summarized as follows.

- We change the unknown and seek the deflection $y_w(T)$ in terms of a new unknown $\rho(\mu,\bar{T})$ as

$$y_w(T) \;=\; a^2\left(\frac{\alpha}{2}\left(\frac{T^2}{a^2}-\frac{1}{12}\right)+\beta\,\rho\left(\mu,\frac{T}{a}\right)\right) \tag{47}$$

  where α, β and μ are parameters depending on strain,

$$\alpha=c-\nu\kappa_2,\quad \beta=\frac{\kappa_2^2\,(c-\nu\kappa_2)-\kappa_2\,\kappa_3^2}{\kappa^{\star 2}},\quad \mu=\left(\frac{\kappa_2}{\kappa^\star}\right)^2\geqslant 0, \tag{48}$$

  and $\kappa^\star$ is the typical strain whose order of magnitude has been anticipated in (4),

$$\kappa^\star=\frac{1}{[12(1-\nu^2)]^{1/2}}\,\frac{t}{a^2}. \tag{49}$$

- Eliminating y_u, y_v and y_w in favor of ρ using (46) and (47), we can rewrite the equilibrium equation (44) as a dimensionless boundary-value problem formulated on the scaled domain $\overline{T}\in(-1/2,+1/2)$,

$$\begin{aligned}&\rho''''(\mu,\overline{T})+\mu\,\rho(\mu,\overline{T})=-\frac{1}{2}\left(\overline{T}^2-\frac{1}{12}\right)\\&\rho''(\mu,\pm1/2)=0,\qquad \rho'''(\mu,\pm1/2)=0.\end{aligned}\tag{50}$$

  The prime $'$ in the equations above stands for differentiation with respect to the argument $\overline{T}$ of ρ. The problem (50) can be solved for $\rho(\mu,\overline{T})$ either numerically or analytically, see Remark 15 below, which completes the solution for y_w. The following equalities can be established directly from the boundary-value problem (50),

$$\int_{-1/2}^{1/2}\rho(\mu,\overline{T})\,\mathrm{d}\overline{T}=0\quad\text{and}\quad\int_{-1/2}^{1/2}\overline{T}\rho(\mu,\overline{T})\,\mathrm{d}\overline{T}=0.\tag{51}$$

  When used in combination with (47), they warrant that the kinematic constraints $\langle y_w(T)\rangle_T=\langle T y_w(T)\rangle_T=0$ in (22) hold.

- The in-plane displacements y_u and y_v are found by integration of (46), the constants of integration being set by the kinematical constraint (22),

$$\begin{aligned}y_u(T)=&-\nu\left(\varepsilon\,T+\frac{\kappa_1}{2}\left(T^2-\frac{a^2}{12}\right)+\frac{\kappa_3^2}{6}T^3\right)+\nu\,\kappa_2\int_0^T y_w(\hat{T})\,\mathrm{d}\hat{T}-\frac{1}{2}\int_0^T(\partial_T y_w(\hat{T}))^2\,\mathrm{d}\hat{T}\\y_v(T)=&\,\kappa_3\left(-2\int_0^T y_w(\hat{T})\,\mathrm{d}\hat{T}+T y_w(T)\right).\end{aligned}\tag{52}$$

In accord with (39), the solution $\boldsymbol{y}=(y_u,y_v,y_w)$ of the problem (38) obtained in (47), (50), and (52) will be denoted as $\boldsymbol{y}=\boldsymbol{Y}^{\boldsymbol{h}}=(Y_u^{\boldsymbol{h}},Y_v^{\boldsymbol{h}},Y_w^{\boldsymbol{h}})$ in the following,

$$y_u=Y_u^{\boldsymbol{h}},\quad y_v=Y_v^{\boldsymbol{h}},\quad y_w=Y_w^{\boldsymbol{h}},\tag{53}$$

where $\boldsymbol{h}=(\varepsilon,\kappa_1,\kappa_2,\kappa_3)$ are the one-dimensional strain measures.

Remark 15. The boundary-value problem (50) has an analytical solution

$$\rho(\mu,\overline{T})=\frac{1}{\mu}\left(\frac{\cos\lambda\overline{T}\cosh\lambda\overline{T}\,(p_1(\lambda)-p_2(\lambda))+\sin\lambda\overline{T}\sinh\lambda\overline{T}\,(p_1(\lambda)+p_2(\lambda))}{\lambda^2(\sin\lambda+\sinh\lambda)}-\frac{1}{2}\left(\overline{T}^2-\frac{1}{12}\right)\right),\tag{54}$$

where $p_1(\lambda)=\cos(\lambda/2)\sinh(\lambda/2)$ and $p_2(\lambda)=\sin(\lambda/2)\cosh(\lambda/2)$ and $\lambda=\mu^{1/4}/\sqrt{2}$. The benefit of this analytical solution is however limited by the fact that the derivatives $\rho_{,\mu}(\mu,\overline{T})$ and $\rho_{,\mu\mu}(\mu,\overline{T})$, which will be needed in the gradient energy terms, have cumbersome expressions: as an alternative to using this analytical solution, one can solve the boundary-value problem (50) numerically for any given value of μ.

4.3. Leading-order strain, pre-stress, and strain energy

Inserting the above solution $\boldsymbol{y}=\boldsymbol{Y}^{\boldsymbol{h}}$ into (43), we get the leading-order expressions of the strain $\boldsymbol{\mathcal{E}}^\star_{[0]}(T;\boldsymbol{h})=\boldsymbol{\mathcal{E}}_{[0]}(T;\boldsymbol{h};\boldsymbol{Y}^{\boldsymbol{h}})$ and stress $\boldsymbol{\Sigma}^\star_{[0]}(T;\boldsymbol{h})=\boldsymbol{K}\boldsymbol{\mathcal{E}}^\star_{[0]}(T;\boldsymbol{h})$ as

$$\boldsymbol{\mathcal{E}}^\star_{[0]}(T;\boldsymbol{h})=\left(\begin{array}{rcl}E_{SS}^{[0]\star}&=&\varepsilon+T\kappa_1-\kappa_2 Y_w^{\boldsymbol{h}}+\frac{(T\kappa_3)^2}{2}\\E_{TT}^{[0]\star}&=&(\cdots)\\E_{ST}^{[0]\star}&=&0\\\hline B_{SS}^{[0]\star}&=&\kappa_2\\B_{TT}^{[0]\star}&=&\partial_{TT}Y_w^{\boldsymbol{h}}-c\\B_{ST}^{[0]\star}&=&-\kappa_3\end{array}\right),\qquad\boldsymbol{\Sigma}^\star_{[0]}(T;\boldsymbol{h})=\left(\begin{array}{rcl}n_{SS}^{[0]\star}&=&Yt\,E_{SS}^{[0]\star}\\n_{TT}^{[0]\star}&=&0\\n_{ST}^{[0]\star}&=&0\\\hline m_{SS}^{[0]\star}&=&D\,(\kappa_2+\nu B_{TT}^{[0]\star})\\m_{TT}^{[0]\star}&=&D\,(\nu\kappa_2+B_{TT}^{[0]\star})\\m_{ST}^{[0]\star}&=&-D(1-\nu)\kappa_3\end{array}\right),\tag{55}$$

where the symbol $(\cdots)$ stands for an expression that is not needed in the following.

Using $(41)_3$ and (28), the strain energy density is $W^\star_{[0]}(\boldsymbol{h})=\int_{-a/2}^{a/2}\frac{1}{2}\boldsymbol{\Sigma}^\star_{[0]}(T;\boldsymbol{h})*\boldsymbol{\mathcal{E}}^\star_{[0]}(T;\boldsymbol{h})\,\mathrm{d}T$ and it can be rewritten as

$$W^\star_{[0]}(\boldsymbol{h})=\int_{-a/2}^{+a/2}\frac{1}{2}\left(n_{SS}^{[0]\star}E_{SS}^{[0]\star}+m_{SS}^{[0]\star}B_{SS}^{[0]\star}+m_{TT}^{[0]\star}B_{TT}^{[0]\star}+2\,m_{ST}^{[0]\star}B_{ST}^{[0]\star}\right)\mathrm{d}T.\tag{56}$$

Inserting the expressions of the stress and strain from (55) and simplifying, see Appendix A, we get the strain energy density as

$$W^\star_{[0]}(\boldsymbol{h})=\frac{Yat}{2}\left(\varepsilon+\frac{a^2\kappa_3^2}{24}\right)^2+\frac{Ya^3t}{2\cdot12}\kappa_1^2+\frac{Yat^3}{2\cdot12}\kappa_2^2+\frac{Yat^3}{2\cdot6\,(1+\nu)}\kappa_3^2+\frac{Ya^5t}{2\cdot2}(\nu\kappa_2^2+\kappa_3^2-c\kappa_2)^2\,\varphi\left(\frac{\kappa_2^2}{\kappa^{\star2}}\right)\tag{57}$$

where $\varphi(\mu)=\frac{1}{360}+2\,\mu\int_{-\frac{1}{2}}^{+\frac{1}{2}}\rho(\mu,\bar{T})\times\frac{1}{2}\left(\bar{T}^2-\frac{1}{12}\right)\mathrm{d}\bar{T}$ has a closed-form expression

$$\varphi(\mu)=\frac{4}{\mu}\left(\frac{1}{2}-\frac{\cosh\lambda-\cos\lambda}{\lambda\,(\sin\lambda+\sinh\lambda)}\right)\quad\text{where}\quad\lambda=\frac{\mu^{1/4}}{\sqrt{2}}. \tag{58}$$

Remark 16. We can further eliminate the strains ε and κ_1 from the energy (57). Minimizing (57) for fixed values of κ_2 and κ_3 gives $\varepsilon=-a^2\,\kappa_3^2/24$ and $\kappa_1=0$. Inserting these values in (57) gives an energy expression similar to that given in the seminal work of Mansfield [9, equation-61]. Mansfield [9] studied tape springs having initial longitudinal curvature and twist: our expression in (57) is a special case of [9] when the initial curvature and twist are set to zero.

Remark 17. The strain energy governing the planar deformations of a tape spring ($\kappa_1=0$ and $\kappa_3=0$) is $W^\star_{[0]\text{planar}}(\varepsilon,\kappa_2)=\frac{1}{2}\,Ya\,t\,\varepsilon^2+\frac{Ya^3t}{2\cdot12}\,\kappa_2^2+\frac{Ya^5t}{2\cdot2}\,(\nu\,\kappa_2^2-c\,\kappa_2)^2\,\varphi(\kappa_2^2/\kappa^{\star 2})$. The constitutive relations for the internal moment M_2 that have been derived in the planar case in [1] are nothing but $M_2=\partial W^\star_{[0]\text{planar}}/\partial\kappa_2$.

Remark 18. Setting the natural curvature c to zero in (57), we recover the extensible ribbon model first derived in [20], see its Equation [2.6]. The energy of a tape spring differs from that of a ribbon only through the $c\,\kappa_2$ term appearing in the squared factor of φ in (57).

Remark 19. The functions $\rho(\mu,\bar{T})$ and $\varphi(\mu)$ in (54) and (58) have *apparent* singularities at $\mu=0$ (*i.e.*, $\lambda=0$). They analytical expressions in (54) and (58) valid for $\mu\neq0$ can be patched with their Taylor expansions around $\mu=0$, namely $\rho(\mu,\bar{T})=\frac{29-420\,\bar{T}^2+560\,\bar{T}^4-448\,\bar{T}^6}{322\,560}+\mu\,\frac{-22\,091+322\,740\,\bar{T}^2+\cdots}{122\,624\,409\,600}+\cdots$ and $\varphi(\mu)=\frac{1}{360}-\frac{\mu}{181\,440}+\cdots$.

5. Higher orders

The leading order solution $\Phi^\star_{[0]}[\boldsymbol{\hbar}]$ in (42) does not capture the gradient effect necessary to accurately predict the localized deformations common in tape springs. In this section, we proceed to derive the first and second order terms $\Phi^\star_{[1]}[\boldsymbol{\hbar}]$ and $\Phi^\star_{[2]}[\boldsymbol{\hbar}]$ of the strain energy functional (1), which depend not only on the macroscopic strain $\boldsymbol{\hbar}(S)$ but also on its gradient $\boldsymbol{\hbar}'(S)$.

5.1. Plan for the higher orders

To calculate the higher order energy terms, the general recipe in [17] introduces an auxiliary strain function $\boldsymbol{e}(T;\boldsymbol{h},\boldsymbol{h}^\dagger,\boldsymbol{h}^\ddagger;\boldsymbol{z},\boldsymbol{z}^\dagger,\boldsymbol{z}^\ddagger)$ defined as

$$\boldsymbol{e}(T;\boldsymbol{h},\boldsymbol{h}^\dagger,\boldsymbol{h}^\ddagger;\boldsymbol{z},\boldsymbol{z}^\dagger,\boldsymbol{z}^\ddagger)=\boldsymbol{\mathcal{E}}(T;\boldsymbol{h},\boldsymbol{h}^\dagger;\boldsymbol{Y}^{\boldsymbol{h}}+\boldsymbol{z},\nabla\boldsymbol{Y}^{\boldsymbol{h}}\cdot\boldsymbol{h}^\dagger+\boldsymbol{z}^\dagger,\boldsymbol{h}^\dagger\cdot\nabla^2\boldsymbol{Y}^{\boldsymbol{h}}\cdot\boldsymbol{h}^\dagger+\nabla\boldsymbol{Y}^{\boldsymbol{h}}\cdot\boldsymbol{h}^\ddagger+\boldsymbol{z}^\ddagger), \tag{59}$$

where $\nabla\boldsymbol{Y}^{\boldsymbol{h}}$, $\nabla^2\boldsymbol{Y}^{\boldsymbol{h}}$ are the first and second derivative (gradient and hessian) of the catalog of leading order solutions $\boldsymbol{Y}^{\boldsymbol{h}}$ with respect to $\boldsymbol{h}$: the ∇ notation stands for differentiation with respect to the one-dimensional strains,

$$\nabla=\frac{\mathrm{d}}{\mathrm{d}\boldsymbol{h}}. \tag{60}$$

In (59), the correction $\boldsymbol{z}$ is a mathematical object of the same type as $\boldsymbol{y}$, *i.e.*, the components (z_u,z_v,z_w) of $\boldsymbol{z}$ are each functions of the single variable T defined on $-a/2\leqslant T\leqslant+a/2$.

Remark 20. The definition (59) can be motivated as follows. Using (35) and (59), we can rewrite the expansion of the microscopic displacement as $\boldsymbol{y}(S)=\boldsymbol{Y}^{\boldsymbol{\hbar}(S)}+\boldsymbol{z}(S)$, where $\boldsymbol{z}(S)=\boldsymbol{y}^\star_{[1]}(S)+\boldsymbol{y}^\star_{[2]}(S)+\cdots$ is the correction to all orders beyond the leading one. The successive derivatives are then given by $\boldsymbol{y}'(S)=\nabla\boldsymbol{Y}^{\boldsymbol{\hbar}(S)}\cdot\boldsymbol{\hbar}'(S)+\boldsymbol{z}'(S)$ and $\boldsymbol{y}''(S)=\boldsymbol{\hbar}'(S)\cdot\nabla^2\boldsymbol{Y}^{\boldsymbol{\hbar}(S)}\cdot\boldsymbol{\hbar}'(S)+\nabla\boldsymbol{Y}^{\boldsymbol{\hbar}(S)}\cdot\boldsymbol{\hbar}''(S)+\boldsymbol{z}(S)$. The strain function $\boldsymbol{e}$ in (59) is nothing but the strain $\boldsymbol{E}=\boldsymbol{e}(T;\boldsymbol{\hbar}(S),\boldsymbol{\hbar}'(S),\boldsymbol{\hbar}''(S);\boldsymbol{z}(S),\boldsymbol{z}'(S),\boldsymbol{z}''(S))$ expressed in terms of $\boldsymbol{\hbar}$, $\boldsymbol{z}$ and their derivatives.

Next, we introduce the *structure coefficients* $\boldsymbol{e}^{ij}_{klm}(T;\boldsymbol{h})$, which are the operators that can be identified from the series expansion of $\boldsymbol{e}$ about the leading order solution $(\boldsymbol{h},\boldsymbol{h}^\dagger,\boldsymbol{h}^\ddagger;\boldsymbol{z},\boldsymbol{z}^\dagger,\boldsymbol{z}^\ddagger)=(\boldsymbol{h},\boldsymbol{0},\boldsymbol{0};\boldsymbol{0},\boldsymbol{0},\boldsymbol{0})$ (see [17, Appendix A3]),

$$\begin{aligned}\boldsymbol{e}(T;\boldsymbol{h},\boldsymbol{h}^\dagger,\boldsymbol{h}^\ddagger;\boldsymbol{z},\boldsymbol{z}^\dagger,\boldsymbol{z}^\ddagger)\;=\;&\boldsymbol{\mathcal{E}}^\star_{[0]}(T;\boldsymbol{h})+\boldsymbol{e}^{10}_{000}(T;\boldsymbol{h})\cdot\boldsymbol{h}^\dagger+(\boldsymbol{e}^{00}_{100}(T;\boldsymbol{h})\cdot\boldsymbol{z})\\&+\frac{1}{2}\,(\boldsymbol{h}^\dagger\cdot\boldsymbol{e}^{20}_{000}(T;\boldsymbol{h})\cdot\boldsymbol{h}^\dagger+2\,\boldsymbol{h}^\dagger\cdot\boldsymbol{e}^{10}_{100}(T;\boldsymbol{h})\cdot\boldsymbol{z}+\boldsymbol{z}\cdot\boldsymbol{e}^{00}_{200}(T;\boldsymbol{h})\cdot\boldsymbol{z})\\&+\boldsymbol{e}^{01}_{000}(T;\boldsymbol{h})\cdot\boldsymbol{h}^\ddagger+\boldsymbol{e}^{00}_{010}(T;\boldsymbol{h})\cdot\boldsymbol{z}^\dagger+\cdots\end{aligned} \tag{61}$$

Inserting the strain expansion (61) into the strain energy, one can get an expansion for the energy. The energy contributions up to second order are listed below, see [17, Appendix A] for details.

$$\begin{aligned}
\boldsymbol{A}(\boldsymbol{h})\cdot\boldsymbol{h}^\dagger &= \int_{-a/2}^{+a/2}\big(\boldsymbol{\Sigma}^\star_{[0]}(T;\boldsymbol{h})*(\boldsymbol{e}^{10}_{000}(T;\boldsymbol{h})\cdot\boldsymbol{h}^\dagger)\big)\,\mathrm{d}T\\
\boldsymbol{C}^{(0)}(\boldsymbol{h})\cdot\boldsymbol{h}^\dagger &= \int_{-a/2}^{+a/2}\big(\boldsymbol{\Sigma}^\star_{[0]}(T;\boldsymbol{h})*(\boldsymbol{e}^{01}_{000}(T;\boldsymbol{h})\cdot\boldsymbol{h}^\dagger)\big)\,\mathrm{d}T\\
\boldsymbol{C}^{(1)}(\boldsymbol{h})\cdot\boldsymbol{z} &= \int_{-a/2}^{+a/2}\big(\boldsymbol{\Sigma}^\star_{[0]}(T;\boldsymbol{h})*(\boldsymbol{e}^{00}_{010}(T;\boldsymbol{h})\cdot\boldsymbol{z})\big)\,\mathrm{d}T\\
\frac{1}{2}\boldsymbol{h}^\dagger\cdot\boldsymbol{B}^{(0)}(\boldsymbol{h})\cdot\boldsymbol{h}^\dagger &= \int_{-a/2}^{+a/2}\Big\{\frac{1}{2}(\boldsymbol{K}(\boldsymbol{e}^{10}_{000}(T;\boldsymbol{h})\cdot\boldsymbol{h}^\dagger))*(\boldsymbol{e}^{10}_{000}(T;\boldsymbol{h})\cdot\boldsymbol{h}^\dagger)\\
&\qquad+\frac{1}{2}\boldsymbol{\Sigma}^\star_{[0]}(T;\boldsymbol{h})*(\boldsymbol{h}^\dagger\cdot\boldsymbol{e}^{20}_{000}(T;\boldsymbol{h})\cdot\boldsymbol{h}^\dagger)\Big\}\,\mathrm{d}T-(\nabla\boldsymbol{C}^{(0)}(\boldsymbol{h})\cdot\boldsymbol{h}^\dagger)\cdot\boldsymbol{h}^\dagger\\
\boldsymbol{h}^\dagger\cdot\boldsymbol{B}^{(1)}(\boldsymbol{h})\cdot\boldsymbol{z} &= \int_{-a/2}^{+a/2}\{(\boldsymbol{K}(\boldsymbol{e}^{10}_{000}(T;\boldsymbol{h})\cdot\boldsymbol{h}^\dagger))*(\boldsymbol{e}^{00}_{100}(T;\boldsymbol{h})\cdot\boldsymbol{z})\\
&\qquad+\boldsymbol{\Sigma}^\star_{[0]}(T;\boldsymbol{h})*(\boldsymbol{h}^\dagger\cdot\boldsymbol{e}^{10}_{100}(T;\boldsymbol{h})\cdot\boldsymbol{z})\}\,\mathrm{d}T-(\nabla\boldsymbol{C}^{(1)}(\boldsymbol{h})\cdot\boldsymbol{h}^\dagger)\cdot\boldsymbol{z}\\
\frac{1}{2}\boldsymbol{z}\cdot\boldsymbol{B}^{(2)}(\boldsymbol{h})\cdot\boldsymbol{z} &= \int_{-a/2}^{+a/2}\Big\{\frac{1}{2}(\boldsymbol{K}(\boldsymbol{e}^{00}_{100}(T;\boldsymbol{h})\cdot\boldsymbol{z}))*(\boldsymbol{e}^{00}_{100}(T;\boldsymbol{h})\cdot\boldsymbol{z})\\
&\qquad+\frac{1}{2}\boldsymbol{\Sigma}^\star_{[0]}(T;\boldsymbol{h})*(\boldsymbol{z}\cdot\boldsymbol{e}^{00}_{200}(T;\boldsymbol{h})\cdot\boldsymbol{z}\Big\}\,\mathrm{d}T
\end{aligned}\tag{62}$$

The $-(\nabla\boldsymbol{C}^{(0)}(\boldsymbol{h})\cdot\boldsymbol{h}^\dagger)\cdot\boldsymbol{h}^\dagger$ and $-(\nabla\boldsymbol{C}^{(1)}(\boldsymbol{h})\cdot\boldsymbol{h}^\dagger)\cdot\boldsymbol{z}$ terms are produced by an integration by parts, the rank-2 tensor $\nabla\boldsymbol{C}^{(0)}(\boldsymbol{h})$ being the gradient of the vector $\boldsymbol{C}^{(0)}(\boldsymbol{h})$ with respect to $\boldsymbol{h}$, see (60). Similarly, $\nabla\boldsymbol{C}^{(1)}(\boldsymbol{h})$ is the gradient with respect to $\boldsymbol{h}$ of the linear operator $\boldsymbol{C}^{(1)}(\boldsymbol{h})$ acting on $\boldsymbol{z}$.

The operators $(\boldsymbol{A}(\boldsymbol{h}),\boldsymbol{C}^{(0)}(\boldsymbol{h}),\boldsymbol{B}^{(0)}(\boldsymbol{h}),\boldsymbol{B}^{(1)}(\boldsymbol{h}),\boldsymbol{B}^{(2)}(\boldsymbol{h}))$ introduced in (62) are all functions of the macroscopic strains $\boldsymbol{h}$. They act on the macroscopic strains gradient $\boldsymbol{h}^\dagger$, microscopic correction $\boldsymbol{z}$ to the displacement and its longitudinal gradient $\boldsymbol{z}^\dagger$. The latter two are still unknown.

According to the general method in [17], the correction $\boldsymbol{z}$ is the solution to the following variational problem on a cross-section, which can be obtained by inserting the expansion of the energy into (32): given $\boldsymbol{h}$ and $\boldsymbol{h}^\dagger$, find a corrector $\boldsymbol{z}$ to the microscopic displacement and Lagrange multipliers $\boldsymbol{f}$ such that

$$\begin{aligned}
\boldsymbol{h}^\dagger\cdot\boldsymbol{B}^{(1)}(\boldsymbol{h})\cdot\hat{\boldsymbol{z}}+\boldsymbol{z}\cdot\boldsymbol{B}^{(2)}(\boldsymbol{h})\cdot\hat{\boldsymbol{z}}-\boldsymbol{f}\cdot\boldsymbol{\mathcal{Q}}\hat{\boldsymbol{z}} &= 0\quad\forall\hat{\boldsymbol{z}}\\
\boldsymbol{\mathcal{Q}}\boldsymbol{z} &= \boldsymbol{0}.
\end{aligned}\tag{63}$$

The variation problem is linear in $\boldsymbol{h}^\dagger$, implying that its solution $\boldsymbol{z}$ is of the form

$$\boldsymbol{z}=\boldsymbol{Z}^{\boldsymbol{h}}\cdot\boldsymbol{h}^\dagger,\tag{64}$$

where $\boldsymbol{Z}^{\boldsymbol{h}}$ is the catalog of corrective displacements. The catalog $\boldsymbol{Z}^{\boldsymbol{h}}$ can be determined by solving the cross-sectional problem (63) for different values $\boldsymbol{h}$.

Inserting the optimal value of $\boldsymbol{z}$ into the energy expansion, we get first and second-order correction to the energy as

$$\begin{aligned}
\Phi^\star_{[1]}[\boldsymbol{\hbar}] &= \int_0^\ell\boldsymbol{A}(\boldsymbol{\hbar}(S))\cdot\boldsymbol{\hbar}'(S)\,\mathrm{d}S\\
\Phi^\star_{[2]}[\boldsymbol{\hbar}] &= \frac{1}{2}\int_0^\ell\boldsymbol{\hbar}'(S)\cdot\boldsymbol{B}(\boldsymbol{\hbar}(S))\cdot\boldsymbol{\hbar}'(S))\,\mathrm{d}S+\Big[\boldsymbol{C}(\boldsymbol{\hbar}(S))\cdot\boldsymbol{\hbar}'(S)\Big]_0^\ell,
\end{aligned}\tag{65}$$

where

$$\begin{aligned}
\boldsymbol{B}(\boldsymbol{h}) &= \boldsymbol{B}^{(0)}_{[0]}(\boldsymbol{h})+2\,\boldsymbol{B}^{(1)}_{[0]}(\boldsymbol{h})\cdot\boldsymbol{Z}^{\boldsymbol{h}}+\boldsymbol{B}^{(2)}_{[0]}(\boldsymbol{h}):(\boldsymbol{Z}^{\boldsymbol{h}}\otimes\boldsymbol{Z}^{\boldsymbol{h}})\big)\\
&= \boldsymbol{B}^{(0)}(\boldsymbol{h})-\boldsymbol{B}^{(2)}(\boldsymbol{h}):(\boldsymbol{Z}^{\boldsymbol{h}}\otimes\boldsymbol{Z}^{\boldsymbol{h}})\\
\boldsymbol{C}(\boldsymbol{h}) &= \boldsymbol{C}^{(0)}(\boldsymbol{h})+\boldsymbol{C}^{(1)}(\boldsymbol{h})\cdot\boldsymbol{Z}^{\boldsymbol{h}}.
\end{aligned}\tag{66}$$

and we used $\boldsymbol{h}^\dagger\cdot\boldsymbol{B}^{(1)}(\boldsymbol{h})\cdot\boldsymbol{z}=-\boldsymbol{z}\cdot\boldsymbol{B}^{(2)}(\boldsymbol{h})\cdot\boldsymbol{z}$ from (63) to simplify $\boldsymbol{B}(\boldsymbol{h})$.

To sum up, the gradient effect can be captured in an asymptotically exact way by identifying the structure coefficients from (61), by defining the operators introduced in (62), by computing the catalog of corrective displacements $\boldsymbol{Z}^{\boldsymbol{h}}$ solving the cross-sectional problem (63), and by using (66) to finally obtain the matrix $\boldsymbol{B}(\boldsymbol{h})$ and the vector $\boldsymbol{C}(\boldsymbol{h})$ entering in the one-dimensional energy (1). The structure coefficients $\boldsymbol{e}^{ij}_{klm}(T;\boldsymbol{h})$ are derived in explicit form in Appendix B, the first-order term $\boldsymbol{A}(\boldsymbol{h})$ entering in $\Phi^\star_{[1]}$ is obtained in (68), and a recipe for calculating numerically the quantities $\boldsymbol{B}(\boldsymbol{h})$ and $\boldsymbol{C}(\boldsymbol{h})$ entering in $\Phi^\star_{[2]}$ is given in Subsection 5.3.

5.2. First-order correction

By inserting into $(62)_1$ the detailed expression of structure coefficients $\boldsymbol{e}^{ij}_{klm}(T;\boldsymbol{h})$ from Appendix B, we obtain

$$\boldsymbol{A}(\boldsymbol{h})\cdot\boldsymbol{h}^\dagger=\int_{-a/2}^{+a/2}[n^{[0]\,\star}_{SS}(\boldsymbol{h})\,\boldsymbol{h}^\dagger\cdot(\nabla Y^{\boldsymbol{h}}_v-T\kappa_3\,\nabla Y^{\boldsymbol{h}}_w)-m^{[0]\,\star}_{SS}(\boldsymbol{h})\,T\kappa_3^\dagger+2\,m^{[0]\,\star}_{ST}(\boldsymbol{h})\,\boldsymbol{h}^\dagger\cdot\partial_T\nabla Y^{\boldsymbol{h}}_w]\,\mathrm{d}T. \tag{67}$$

In the right-hand side of (67), $n^{[0]\,\star}_{\alpha\beta}(\boldsymbol{h})$ and $m^{[0]\,\star}_{\alpha\beta}(\boldsymbol{h})$ denote the pre-stress predicted by the leading-order solution, see $(55)_2$, $Y^{\boldsymbol{h}}_i$ denotes the components from the catalog of microscopic displacement at leading order ($i\in\{w,u,v\}$), see (53), $\nabla Y^{\boldsymbol{h}}_i$ denote their gradient with respect to $\boldsymbol{h}$, see (60). As usual, the strain κ_3 and its gradient $\kappa_3^\dagger$ in the right-hand side are related to the symbols in the left-hand side through $\boldsymbol{h}=(\varepsilon,\kappa_1,\kappa_2,\kappa_3)$ and $\boldsymbol{h}^\dagger=(\varepsilon^\dagger,\kappa_1^\dagger,\kappa_2^\dagger,\kappa_3^\dagger)$.

This expression (67) can be simplified using symmetry considerations as follows. The solution $\rho(\mu,\overline{T})$ of the boundary-value problem (50) is an even function of $\overline{T}$. As a result, the deflection $Y^{\boldsymbol{h}}_w(T)$ in (47) is also an even function of T. Equation (55) further shows that $B^{[0]\,\star}_{TT}$ and $m^{[0]\,\star}_{SS}$ are both even functions of T. The symmetry of the integration domain $T\in[-a/2,+a/2]$ implies that the second term in the integrand (67) is odd, and therefore integrates out to zero, $\int_{-a/2}^{+a/2}-m^{[0]\,\star}_{SS}(\boldsymbol{h})\,T\kappa_3^\dagger\,\mathrm{d}T=0$. A similar argument holds for the last term in the integrand: Equation (55) shows that $m^{[0]\,\star}_{ST}$ is independent of T and $\partial_T\nabla Y^{\boldsymbol{h}}_w$ is an odd function of T, so that $\int_{-a/2}^{+a/2}2\,m^{[0]\,\star}_{ST}(\boldsymbol{h})\,\boldsymbol{h}^\dagger\cdot\partial_T\nabla Y^{\boldsymbol{h}}_w\,\mathrm{d}T=0$. The first term in the integrand of (67) can be simplified as follows. Equation (55) shows that the first factor, $n^{[0]\,\star}_{SS}(\boldsymbol{h})$, is equal to $Yt\,T\kappa_1$ plus an even function of T. In view of $(52)_2$, $Y^{\boldsymbol{h}}_v(T)$ is an odd function of T, implying that the other factor in the first term, $\nabla Y^{\boldsymbol{h}}_v-T\kappa_3\,\nabla Y^{\boldsymbol{h}}_w$, is an odd function of T. After dropping the terms that integrate out to zero, this leaves us with

$$\boldsymbol{A}(\boldsymbol{h})\cdot\boldsymbol{h}^\dagger=Yt\,\kappa_1\,\boldsymbol{h}^\dagger\cdot\int_{-a/2}^{+a/2}T\,(\nabla Y^{\boldsymbol{h}}_v-T\kappa_3\,\nabla Y^{\boldsymbol{h}}_w)\,\mathrm{d}T. \tag{68}$$

The energy correction $\Phi^\star_{[1]}[\boldsymbol{\hbar}]$ follows from $(65)_1$.

Remark 21. In both the planar case ($\kappa_1=\kappa_3=0$) and in the case of no bending ($\kappa_1=\kappa_2=0$, see Section C in the Appendix), we have $\boldsymbol{A}(\boldsymbol{h})\cdot\boldsymbol{h}^\dagger=0$, and therefore $\Phi^\star_{[1]}[\boldsymbol{\hbar}]=0$.

5.3. Second-order correction

An explicit form of the operators $\boldsymbol{C}^{(0)}$ and $\boldsymbol{C}^{(1)}$ appearing in (62) can be found by inserting the expressions of the structure coefficients $\boldsymbol{e}^{ij}_{klm}(T;\boldsymbol{h})$ from Appendix B and of the stress $\boldsymbol{\Sigma}^\star_{[0]}$ from $(55)_2$,

$$\begin{aligned}\boldsymbol{C}^{(0)}(\boldsymbol{h})\cdot\boldsymbol{h}^\dagger &= \int_{-a/2}^{+a/2}\big(m^{[0]\,\star}_{SS}(\boldsymbol{h})\,\boldsymbol{h}^\dagger\cdot\nabla Y^{\boldsymbol{h}}_w\big)\,\mathrm{d}T\\ \boldsymbol{C}^{(1)}(\boldsymbol{h})\cdot\boldsymbol{z} &= \int_{-a/2}^{+a/2}\Big(n^{[0]\,\star}_{SS}(\boldsymbol{h})\,(z_v-T\kappa_3\,z_w)+2\,m^{[0]\,\star}_{ST}(\boldsymbol{h})\,\partial_T z_w\Big)\,\mathrm{d}T\end{aligned} \tag{69}$$

The expressions of the $\boldsymbol{B}^{(i)}$ operators are obtained similarly. This yields the operator independent of $\boldsymbol{z}$ as

$$\begin{aligned}\frac{1}{2}\boldsymbol{h}^\dagger\cdot\boldsymbol{B}^{(0)}(\boldsymbol{h})\cdot\boldsymbol{h}^\dagger=\int_{-a/2}^{+a/2}\Bigg\{&\frac{K}{2}\left(\begin{array}{l}(\boldsymbol{h}^\dagger\cdot(\nabla Y^{\boldsymbol{h}}_v-T\kappa_3\,\nabla Y^{\boldsymbol{h}}_w))^2\\ +2\,(1-\nu)\left(\dfrac{\boldsymbol{h}^\dagger}{2}\cdot(\nabla Y^{\boldsymbol{h}}_u+\nabla Y^{\boldsymbol{h}}_w\,\partial_T Y^{\boldsymbol{h}}_w)\right)^2\end{array}\right)\\ &+\frac{D}{2}\Big((T\kappa_3^\dagger)^2+2\,(1-\nu)\,(\boldsymbol{h}^\dagger\cdot\nabla\partial_T Y^{\boldsymbol{h}}_w)^2\Big)+n^{[0]\,\star}_{SS}(\boldsymbol{h})\,\frac{\boldsymbol{h}^\dagger\cdot(\nabla Y^{\boldsymbol{h}}_w\otimes\nabla Y^{\boldsymbol{h}}_w)\cdot\boldsymbol{h}^\dagger}{2}+m^{[0]\,\star}_{SS}\,\boldsymbol{h}^\dagger\cdot\nabla^2 Y^{\boldsymbol{h}}_w\cdot\boldsymbol{h}^\dagger\\ &-\boldsymbol{h}^\dagger\cdot(\nabla m^{[0]\,\star}_{SS}(\boldsymbol{h})\otimes\nabla Y^{\boldsymbol{h}}_w+m^{[0]\,\star}_{SS}(\boldsymbol{h})\,\nabla^2 Y^{\boldsymbol{h}}_w)\cdot\boldsymbol{h}^\dagger\Bigg\}\,\mathrm{d}T,\end{aligned} \tag{70}$$

the operator linear in $\boldsymbol{z}$ as

$$\begin{aligned}\boldsymbol{h}^\dagger\cdot\boldsymbol{B}^{(1)}(\boldsymbol{h})\cdot\boldsymbol{z}=\int_{-a/2}^{+a/2}\Bigg\{&K\left(\boldsymbol{h}^\dagger\cdot(\nabla Y^{\boldsymbol{h}}_v-T\kappa_3\,\nabla Y^{\boldsymbol{h}}_w)\,(-\kappa_2\,z_w+\nu\,(\partial_T z_u+\partial_T Y^{\boldsymbol{h}}_w\,\partial_T z_w))\right)\\ &+2\,K\,(1-\nu)\left(\frac{\boldsymbol{h}^\dagger\cdot(\nabla Y^{\boldsymbol{h}}_u+\nabla Y^{\boldsymbol{h}}_w\,\partial_T Y^{\boldsymbol{h}}_w)}{2}\,\frac{(\partial_T z_v+\kappa_3\,(z_w-T\partial_T z_w))}{2}\right)\\ &-D\,\nu T\kappa_3{}^\dagger\,\partial_{TT}z_w-\left(\begin{array}{l}\boldsymbol{h}^\dagger\cdot\nabla n^{[0]\,\star}_{SS}(\boldsymbol{h})\,(z_v-T\kappa_3\,z_w)\\ -n^{[0]\,\star}_{SS}(\boldsymbol{h})\,T\kappa_3^\dagger\,z_w+2\,\boldsymbol{h}^\dagger\cdot\nabla m^{[0]\,\star}_{ST}(\boldsymbol{h})\,\partial_T z_w\end{array}\right)\Bigg\}\,\mathrm{d}T,\end{aligned} \tag{71}$$

and the one quadratic in $\boldsymbol{z}$ as

$$\begin{aligned}\frac{1}{2}\boldsymbol{z}\cdot\boldsymbol{B}^{(2)}(\boldsymbol{h})\cdot\boldsymbol{z}=\frac{1}{2}\int_{-a/2}^{+a/2}\Big\{&K\left((\kappa_2\,z_w)^2+(\partial_T z_u+\partial_T Y_w^{\boldsymbol{h}}\,\partial_T z_w)^2\right)\\&+2\,K\,(1-\nu)\left(\frac{(\partial_T z_v+\kappa_3\,(z_w-T\,\partial_T z_w))}{2}\right)^2-2\,K\,\nu\,\kappa_2\,z_w\,(\partial_T z_u+\partial_T Y_w^{\boldsymbol{h}}\,\partial_T z_w)+D\,(\partial_{TT} z_w)^2\Big\}\mathrm{d}T\end{aligned}\tag{72}$$

These definitions are complete and self-contained: the arguments $\boldsymbol{z}$, $\boldsymbol{h}$ and $\boldsymbol{h}^\dagger$ are dummy arguments, and all the other quantities appearing in the right-hand sides can be derived from the leading-order solution from Section 4 with the help of the diagram in Figure 2.

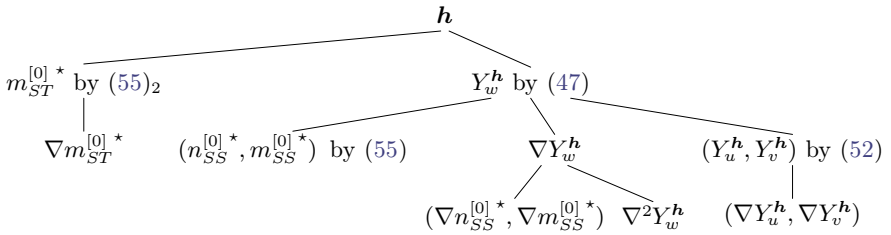

Figure 2. Dependency diagram showing how the auxiliary quantities entering in the definition of the operators $\boldsymbol{A}(\boldsymbol{h})$, $\boldsymbol{C}^{(i)}(\boldsymbol{h})$ and $\boldsymbol{B}^{(i)}(\boldsymbol{h})$ can be obtained in terms of $\boldsymbol{h}$. To compute $\nabla n_{SS}^{[0]\star}$, for instance, one should differentiate (55) with respect to $\boldsymbol{h}$ symbolically: the result depends on $\nabla Y_w^{\boldsymbol{h}}$ which can in turn be obtained by differentiating (47) symbolically or numerically with respect to $\boldsymbol{h}$.

In the diagram, the quantity $\nabla Y_w^{\boldsymbol{h}}=\frac{\mathrm{d}Y_w^{\boldsymbol{h}}}{\mathrm{d}\boldsymbol{h}}$ is obtained by differentiating (47) as

$$\nabla Y_w^{\boldsymbol{h}}(T)=a^2\left(\frac{\nabla\alpha(\boldsymbol{h})}{2}\left(\left(\frac{T}{a}\right)^2-\frac{1}{12}\right)+\nabla\beta(\boldsymbol{h})\,\rho\Big(\mu(\boldsymbol{h}),\frac{T}{a}\Big)+\rho(\boldsymbol{h})\,\nabla\mu(\boldsymbol{h})\,\rho_{,\mu}\Big(\mu(\boldsymbol{h}),\frac{T}{a}\Big)\right).$$

where the quantities $\nabla\alpha(\boldsymbol{h})$, $\nabla\beta(\boldsymbol{h})$ and $\nabla\mu(\boldsymbol{h})$ are readily obtained from (48), and the auxiliary function $\rho_{,\mu}$ can be calculated by solving the boundary-value problem obtained by differentiating (50) with respect to μ or by a symbolic differentiation of the closed-form solution (54) for ρ with respect to μ. The second gradient $\nabla^2 Y_w^{\boldsymbol{h}}(T)$ can be obtained by differentiating one more time.

Having obtained the operators $\boldsymbol{B}^{(1)}(\boldsymbol{h})$ and $\boldsymbol{B}^{(2)}(\boldsymbol{h})$, one can proceed to solve the problem (63) yielding the correction $\boldsymbol{z}$ to the microscopic displacement. This delivers the second catalog $\boldsymbol{Z}^{\boldsymbol{h}}$ appearing in (64), for any value of $\boldsymbol{h}$. Inserting into (66), one obtains the matrix $\boldsymbol{B}(\boldsymbol{h})$ and the vector $\boldsymbol{C}(\boldsymbol{h})$ for any particular value of $\boldsymbol{h}$. This completes the calculation of the energy contribution $\Phi_{[2]}^\star$.

Remark 22. The operators that do not depend on $\boldsymbol{z}$ are $\boldsymbol{A}(\boldsymbol{h})$ (a vector of length 4), $\boldsymbol{C}^{(0)}(\boldsymbol{h})$ (a vector of length 4), and $\boldsymbol{B}^{(0)}(\boldsymbol{h})$ (a matrix with dimensions 4×4). The other operators act on $\boldsymbol{z}$ and are therefore functionals. They are naturally represented in the computer using finite-elements over a one-dimensional mesh for the T-domain $[-a/2,+a/2]$. This entails expressing the three functions $\boldsymbol{z}=(z_u,z_v,z_w)$ in terms of discrete degrees of freedom and constructing matrices representing $\boldsymbol{C}^{(1)}(\boldsymbol{h})$, $\boldsymbol{B}^{(1)}(\boldsymbol{h})$ and $\boldsymbol{B}^{(2)}(\boldsymbol{h})$ through a standard assembly process. This assembly should be done for a fixed value of $\boldsymbol{h}$. An alternative to this numerical approach is the symbolic approach illustrated in Section C in the Appendix for the case of no bending, which is not tractable in the general case.

In summary, the dimension reduction involves the solution of two variational problems formulated on a cross-section: the non-linear variational problem (38) for the leading-order displacement $\boldsymbol{y}$ (which we have managed to solve analytically in Subsection 4.2), and the solution of the linear variational problem (63) for the higher-order correction $\boldsymbol{z}$.

6. Concluding remarks

We have obtained a one-dimensional strain energy functional for tape springs. Equilibrium configurations of tape springs are stationary points of this energy functional (1) plus a potential representing the external loading, subjected to the kinematic constraints in (6), (12), and (13). The equilibrium configurations can be computed using the finite element method, the discrete elastic rod method [5], or standard differential equation solvers. Note that most solvers, no matter if they use the weak or strong form of the equilibrium, may require the evaluation of the gradients $\nabla^k\boldsymbol{A}(\boldsymbol{h})$, $\nabla^k\boldsymbol{B}(\boldsymbol{h})$ and $\nabla^k\boldsymbol{C}(\boldsymbol{h})$, whose implementation we have not discussed here.

An important open question concerns the positive-definite character of the symmetric matrix $\boldsymbol{B}(\boldsymbol{h})$ providing the strain-gradient regularization. In the related context of higher-order homogenization, $\boldsymbol{B}$ has been found to have negative eigenvalues, see for instance [24, Section 4.3]: in such circumstances, the regularized energy $\Phi^\star$ can be made arbitrarily large and negative by solutions featuring small-amplitude, fine-scale oscillations of the strain. To work around this, it has been suggested in [24] to reset the negative eigenvalues of $\boldsymbol{B}$ to zero. This point deserves further attention.

Our model for tape springs can be particularized to ribbons by setting the initial transverse curvature to zero, $c=0$. This special case is interesting as there exists no ribbon model to date that takes both extensibility and the gradient effect into account, although both are known to play an important role in the deformation of elastic ribbons, see for instance [20]. Besides, numerical models for tape springs and ribbons are not available in commercial software or open-source libraries. A numerical implementation of the proposed model, its validation using experiments and two-dimensional shell simulations, and its distribution as an open-source libraries will be covered in follow-up papers.

Sections 3, 4, and 5 presented a generalized tape spring model including all four strains $(\varepsilon,\kappa_1,\kappa_2,\kappa_3)$. One can condense out the stiff modes ε (stretching) and κ_1 (bending) by minimizing the leading order strain energy $\Phi^\star_{[0]}$ in (57) with respect to ε and κ_1, as mentioned in Remark 16 and done in [20]. This gives optimal values of $\varepsilon=-a^2\kappa_3^2/24$ and $\kappa_1=0$. In principle, by inserting these relations into the gradient terms from Section 5, one can eliminate stretch and transverse bending from the energy entirely and obtain a simple one-dimensional model for tape springs. This will be covered in future work.

The strain energy functional $\Phi^\star$ obtained in the paper can be used without any modification to produce dynamic simulations of tape springs, thereby allowing fast and accurate simulations of the deployment of tape springs for instance [1]. Dynamic applications of our one-dimensional model is another interesting line of research that will be explored in future work.

Acknowledgment

Arun Kumar is supported by the Europostdoc2 Marie Curie fellowship receiving funding from the European Union's Horizon 2020 research and innovation program under the Marie Sklodowska Curie grant agreement no. 899987.

Appendix A. Leading-order energy calculation

The leading order strain energy density $W^\star_{[0]}(\boldsymbol{h})$ given in (57) and the definition of the auxiliary function ρ in (58) can be justified as follows.

The strain energy in $(41)_3$ can be rewritten with the help of (28) and (55) as the sum of a stretching energy and a bending energy, $W^\star_{[0]}(\boldsymbol{h})=W^\star_{[0],\mathrm{s}}(\boldsymbol{h})+W^\star_{[0],\mathrm{b}}(\boldsymbol{h})$ where

$$W^\star_{[0],\mathrm{s}}(\boldsymbol{h})=\int_{-a/2}^{+a/2}\frac{n^{[0]\,\star}_{SS}\,E^{[0]\,\star}_{SS}}{2}\,\mathrm{d}T\quad\text{and}\quad W^\star_{[0],\mathrm{b}}(\boldsymbol{h})=\int_{-a/2}^{+a/2}\frac{m^{[0]\,\star}_{SS}\,B^{[0]\,\star}_{SS}+m^{[0]\,\star}_{TT}\,B^{[0]\,\star}_{TT}+2\,m^{[0]\,\star}_{ST}\,B^{[0]\,\star}_{ST}}{2}\,\mathrm{d}T.$$

Using successively (55), (47) and (48) the stretching energy can be written as

$$\begin{aligned}
W^\star_{[0],\mathrm{s}}(\boldsymbol{h}) &= \frac{Yt}{2}\int_{-a/2}^{+a/2}\left(\varepsilon+T\kappa_1+\frac{1}{2}(T\kappa_3)^2-\kappa_2\,Y^{\boldsymbol{h}}_w\right)^2\mathrm{d}T\\
&= \frac{Yt}{2}\int_{-a/2}^{+a/2}\left(\varepsilon+\frac{a^2\kappa_3^2}{24}+T\kappa_1+\frac{a^2\kappa_3^2}{2}\left(\frac{T^2}{a^2}-\frac{1}{12}\right)-\kappa_2\,a^2\left(\frac{\alpha}{2}\left(\frac{T^2}{a^2}-\frac{1}{12}\right)+\beta\rho\right)\right)^2\mathrm{d}T\\
&= \frac{Yt}{2}\int_{-a/2}^{+a/2}\left(\left(\varepsilon+\frac{a^2\kappa_3^2}{24}\right)+T\kappa_1-a^2\,\kappa_2\,\beta\left(\rho+\frac{1}{2\,\mu}\left(\frac{T^2}{a^2}-\frac{1}{12}\right)\right)\right)^2\mathrm{d}T
\end{aligned}$$

Here, $\alpha=\alpha(\boldsymbol{h})$, $\beta=\beta(\boldsymbol{h})$, and $\mu=\mu(\boldsymbol{h})$ denote the strain parameters introduced in (48) and $\rho=\rho\left(\frac{\kappa_2^2}{\kappa^{\star 2}},\frac{T}{a}\right)$.

Expanding the square, integrating, and using (51) we have

$$\begin{aligned}
W^\star_{[0],\mathrm{s}}(\boldsymbol{h}) &= \frac{Yt}{2}\int_{-a/2}^{+a/2}\left[\left(\varepsilon+\frac{a^2\kappa_3^2}{24}\right)^2+T^2\kappa_1^2+(a^2\kappa_2\,\beta)^2\left(\rho+\frac{1}{2\,\mu}\left(\frac{T^2}{a^2}-\frac{1}{12}\right)\right)^2\right]\mathrm{d}T\\
&= \frac{Yat}{2}\left[\left(\varepsilon+\frac{a^2\kappa_3^2}{24}\right)^2+\frac{a^2\kappa_1^2}{12}+(a^2\kappa_2\,\beta)^2\left\langle\left(\rho+\frac{1}{2\,\mu}\left(\frac{T^2}{a^2}-\frac{1}{12}\right)\right)^2\right\rangle_T\right].
\end{aligned}\tag{73}$$

The bending energy can be rewritten with the help of (55) as

$$\begin{aligned}
W^\star_{[0],\mathrm{b}}(\boldsymbol{h}) &= \frac{D}{2}\int_{-a/2}^{+a/2}(\kappa_2\,(\kappa_2+\nu\,B^{[0]\,\star}_{TT})+B^{[0]\,\star}_{TT}\,(\nu\,\kappa_2+B^{[0]\,\star}_{TT})+2\,(1-\nu)\,\kappa_3^2)\,\mathrm{d}T\\
&= \frac{D}{2}\int_{-a/2}^{+a/2}((B^{[0]\,\star}_{TT}+\nu\,\kappa_2)^2+(1-\nu^2)\,\kappa_2^2+2\,(1-\nu)\,\kappa_3^2)\,\mathrm{d}T.
\end{aligned}$$

Using (55), (47) and (48), we have $B^{[0]\,\star}_{TT}+\nu\kappa_2=\partial_{TT}Y^{\boldsymbol{h}}_w-c+\nu\kappa_2=\alpha-c+\beta\rho''+\nu\kappa_2=\beta\rho''$ where we use the shorthand $\rho''=\frac{\partial^2\rho}{\partial\bar{T}^2}(\mu,T/a)$. Inserting into the equation above and integrating, we get

$$W^\star_{[0],\mathrm{b}}(\boldsymbol{h})=\frac{D\,a}{2}\,(\beta^2\,\langle\rho''^2\rangle_T+(1-\nu^2)\,\kappa_2^2+2\,(1-\nu)\,\kappa_3^2). \tag{74}$$

The sum $W^\star_{[0]}(\boldsymbol{h})=W^\star_{[0],\mathrm{s}}(\boldsymbol{h})+W^\star_{[0],\mathrm{b}}(\boldsymbol{h})$ of the bending and stretching energies in (73) and (74) is consistent with that announced in (57) provided we identify the remaining terms as follows

$$\frac{Ya\,t}{2}\,(a^2\,\kappa_2\,\beta)^2\left\langle\left(\rho+\frac{1}{2\,\mu}\left(\frac{T^2}{a^2}-\frac{1}{12}\right)\right)^2\right\rangle_T+\frac{D\,a}{2}\,\beta^2\,\langle\rho''^2\rangle_T\equiv\frac{Ya^5\,t}{2\cdot2}\,\frac{\beta^2\,\kappa^{\star2}}{\mu}\,\varphi$$

Using $D=Yt\,(a^2\,\kappa^\star)^2$ and simplifying, this yields the following definition of the auxiliary function φ,

$$\varphi=\left\langle 2\,\mu\,\rho''^2+2\left(\mu\,\rho+\frac{1}{2}\left(\frac{T^2}{a^2}-\frac{1}{12}\right)\right)^2\right\rangle_T$$

Multiplying both sides of $(50)_1$ by ρ, integrating twice by parts and using the boundary conditions $(50)_2$, one can establish the identity $\left\langle\rho''^2+\mu\,\rho^2+\frac{\rho}{2}\left(\frac{T^2}{a^2}-\frac{1}{12}\right)\right\rangle_T=0$, which we can then use to eliminate the ρ''^2 term from the definition of φ. The result is

$$\varphi=\frac{1}{360}+2\,\mu\left\langle\rho\times\frac{1}{2}\left(\frac{T^2}{a^2}-\frac{1}{12}\right)\right\rangle_T.$$

This is precisely the definition of φ that has been used above Equation (58).

Appendix B. Structure coefficients

The strain variant $\boldsymbol{e}(T;\boldsymbol{h},\boldsymbol{h}^\dagger,\boldsymbol{h}^\ddagger;\boldsymbol{z},\boldsymbol{z}^\dagger,\boldsymbol{z}^\ddagger)$ given in (59) is calculated as

$$\boldsymbol{e}(T;\boldsymbol{h},\boldsymbol{h}^\dagger,\boldsymbol{h}^\ddagger;\boldsymbol{z},\boldsymbol{z}^\dagger,\boldsymbol{z}^\ddagger)=\left(\begin{array}{c}\varepsilon+T\kappa_1-\kappa_2\,(Y^{\boldsymbol{h}}_w+z_w)+\boldsymbol{h}^\dagger\cdot\nabla Y^{\boldsymbol{h}}_v+z^\dagger_v+\frac{1}{2}\,(-T\kappa_3+\boldsymbol{h}^\dagger\cdot\nabla Y^{\boldsymbol{h}}_w+z^\dagger_w)^2\\ \partial_T Y^{\boldsymbol{h}}_u+\partial_T z_u+\frac{1}{2}\,(\partial_T Y^{\boldsymbol{h}}_w+\partial_T z_w)^2\\ \frac{1}{2}\left(\begin{array}{r}\kappa_3\,(Y^{\boldsymbol{h}}_w+z_w-T\,(\partial_T Y^{\boldsymbol{h}}_w+\partial_T z_w))+\partial_T Y^{\boldsymbol{h}}_v+\partial_T z_v+\boldsymbol{h}^\dagger\cdot\nabla Y^{\boldsymbol{h}}_u+z^\dagger_u\cdot\cdots\\ +(\boldsymbol{h}^\dagger\cdot\nabla Y^{\boldsymbol{h}}_w+z^\dagger_w)\,(\partial_T Y^{\boldsymbol{h}}_w+\partial_T z_w)\end{array}\right)\\ \hline \kappa_2-T\kappa_3^\dagger+\boldsymbol{h}^\ddagger\cdot\nabla Y^{\boldsymbol{h}}_w+\boldsymbol{h}^\dagger\cdot\nabla^2 Y^{\boldsymbol{h}}_w\cdot\boldsymbol{h}^\dagger+z^\ddagger_w\\ \partial_{TT}Y^{\boldsymbol{h}}_w+\partial_{TT}z_w-c\\ -\kappa_3+\boldsymbol{h}^\dagger\cdot\nabla\partial_T Y^{\boldsymbol{h}}_w+\partial_T z^\dagger_w\end{array}\right)$$

The structure coefficients $\boldsymbol{e}^{ij}_{klm}(T;\boldsymbol{h})$ can be identified from the Taylor expansion of $\boldsymbol{e}$ as follows, see (61),

$$\begin{aligned}
\boldsymbol{e}^{10}_{000}(T;\boldsymbol{h})\cdot\boldsymbol{h}^\dagger&=\left(\begin{array}{ccc|ccc}\boldsymbol{h}^\dagger\cdot(\nabla Y^{\boldsymbol{h}}_v-T\kappa_3\,\nabla Y^{\boldsymbol{h}}_w) & 0 & \frac{1}{2}\,\boldsymbol{h}^\dagger\cdot(\nabla Y^{\boldsymbol{h}}_u+\nabla Y^{\boldsymbol{h}}_w\,\partial_T Y^{\boldsymbol{h}}_w) & -T\kappa_3^\dagger & 0 & \boldsymbol{h}^\dagger\cdot\nabla\partial_T Y^{\boldsymbol{h}}_w\end{array}\right)\\
\frac{1}{2}\,\boldsymbol{h}^\dagger\cdot\boldsymbol{e}^{20}_{000}(T;\boldsymbol{h})\cdot\boldsymbol{h}^\dagger&=\left(\begin{array}{ccc|ccc}\boldsymbol{h}^\dagger\cdot\frac{\nabla Y^{\boldsymbol{h}}_w\otimes\nabla Y^{\boldsymbol{h}}_w}{2}\cdot\boldsymbol{h}^\dagger & 0 & 0 & \boldsymbol{h}^\dagger\cdot\nabla^2 Y^{\boldsymbol{h}}_w\cdot\boldsymbol{h}^\dagger & 0 & 0\end{array}\right)\\
\boldsymbol{h}^\dagger\cdot\boldsymbol{e}^{10}_{100}(T;\boldsymbol{h})\cdot\boldsymbol{z}&=\left(\begin{array}{ccc|ccc}0 & 0 & \frac{1}{2}\,\partial_T z_w\,\boldsymbol{h}^\dagger\cdot\nabla Y^{\boldsymbol{h}}_w & 0 & 0 & 0\end{array}\right)\\
\boldsymbol{e}^{00}_{100}(T;\boldsymbol{h})\cdot\boldsymbol{z}&=\left(\begin{array}{ccc|ccc}-\kappa_2\,z_w & \partial_T z_u+\partial_T Y^{\boldsymbol{h}}_w\,\partial_T z_w & \frac{1}{2}\,(\partial_T z_v+\kappa_3\,(z_w-T\partial_T z_w)) & 0 & \partial_{TT}z_w & 0\end{array}\right)\\
\boldsymbol{e}^{01}_{000}(T;\boldsymbol{h})\cdot\boldsymbol{h}^\ddagger&=\left(\begin{array}{ccc|ccc}0 & 0 & 0 & \boldsymbol{h}^\ddagger\cdot\nabla Y^{\boldsymbol{h}}_w & 0 & 0\end{array}\right)\\
\frac{1}{2}\,\boldsymbol{z}\cdot\boldsymbol{e}^{00}_{200}(T;\boldsymbol{h})\cdot\boldsymbol{z}&=\left(\begin{array}{ccc|ccc}0 & \frac{1}{2}\,(\partial_T z_w)^2 & 0 & 0 & 0 & 0\end{array}\right)\\
\boldsymbol{e}^{00}_{010}(T;\boldsymbol{h})\cdot\boldsymbol{z}^\dagger&=\left(\begin{array}{ccc|ccc}z^\dagger_v-T\kappa_3\,z^\dagger_w & 0 & \frac{1}{2}\,(z^\dagger_u+\partial_T Y^{\boldsymbol{h}}_w\,z^\dagger_w) & 0 & 0 & \partial_T z^\dagger_w\end{array}\right)
\end{aligned} \tag{75}$$

Appendix C. The special case of no bending

In this Appendix, we specialize our analysis to deformations of the tape spring involving no bending ($\kappa_1=\kappa_2=0$). This special case provides simpler version of the general theory presented in this paper, and is meant to illustrate how it works.

For $\kappa_1=\kappa_2=0$, the cross-sectional displacements that are solutions of the leading-order boundary-value problem in (44) and (45) can be found as

$$Y^{\boldsymbol{h}}_u=-T\nu\,\varepsilon-\frac{T^3}{6}(c^2+\kappa_3^2),\qquad Y^{\boldsymbol{h}}_v=\frac{c\,T}{24}\,(a^2+4\,T^2)\,\kappa_3,\qquad Y^{\boldsymbol{h}}_w=\frac{c}{2}\left(T^2-\frac{a^2}{12}\right). \tag{76}$$

These expressions can also be obtained by taking the limits $\kappa_1 \to 0$ and $\kappa_2 \to 0$ in the general solution in (46) and (52). What makes the no-bending case simpler is that these expressions are polynomial in T—compare to general case in (47) and (54).

The strain and stress components appearing in (55) are then given by

$$\begin{array}{llll} E_{SS}^{[0]\star} = \varepsilon + \dfrac{(T\kappa_3)^2}{2}, & B_{SS}^{[0]\star} = 0, & B_{TT}^{[0]\star} = 0, & B_{ST}^{[0]\star} = -\kappa_3 \\ n_{SS}^{[0]\star} = Yt\left(\varepsilon + \dfrac{(T\kappa_3)^2}{2}\right), & m_{SS}^{[0]\star} = 0, & m_{TT}^{[0]\star} = 0, & m_{ST}^{[0]\star} = -\dfrac{Yt^3}{12(1+\nu)}\kappa_3. \end{array} \tag{77}$$

Inserting into (56), we obtain the leading-order contribution to the strain energy as

$$\Phi^\star_{[0]}[\boldsymbol{\hbar}] \;=\; \int_0^\ell \left[\frac{1}{2} Ya\,t\left(\varepsilon(S) + \frac{a^2\,\kappa_3^2(S)}{24}\right)^2 + \frac{Ya\,t^3}{2\cdot 6\,(1+\nu)}\kappa_3^2(S) + \frac{Ya^5\,t}{2\cdot 2\cdot 360}\kappa_3^4(S)\right]\,\mathrm{d}S.$$

The same result can alternatively be obtained by taking the limit $(\kappa_1, \kappa_2) \to \mathbf{0}$ of the general expression of $\Phi^\star_{[0]}$ given in (57), noting that $\varphi(0) = 1/360$ (see Remark 19).

Given that $\kappa_1 = 0$, Equation (68) yields

$$\boldsymbol{A}(\boldsymbol{\hbar}(S)) \cdot \boldsymbol{\hbar}'(S)\,\mathrm{d}S = 0.$$

The gradients with respect to the strain $\boldsymbol{h}$ of the leading-order displacement in (76) is obtained as $\nabla Y_w^{\boldsymbol{h}} = \mathbf{0}$, $\nabla^2 Y_w^{\boldsymbol{h}} = \mathbf{0}$, $\nabla Y_u^{\boldsymbol{h}} = \begin{pmatrix} -T\nu & 0 & 0 & -T^3\kappa_3/3 \end{pmatrix}$, etc. Those of the leading-order stress in (77) are obtained similarly as $\nabla n_{SS}^{[0]\star} = \begin{pmatrix} Yt & 0 & 0 & Yt\,T^2\kappa_3 \end{pmatrix}$ and $\nabla m_{ST}^{[0]\star} = \begin{pmatrix} 0 & 0 & 0 & -\frac{Yt^3}{12(1+\nu)} \end{pmatrix}$. Inserting into the operators $\boldsymbol{B}^{(1)}$ and $\boldsymbol{B}^{(2)}$ in (71) and (72), we can rewrite the variational problem (63) for $\boldsymbol{z}$ as follows: find three functions (z_u, z_v, z_w) of the single variable T satisfying the zero-average conditions $\boldsymbol{\mathcal{Q}}\boldsymbol{z} = \mathbf{0}$, as well as four numbers $(f_S, f_T, f_\mathrm{n}, f_\mathrm{t})$, such that

$$\int_{-a/2}^{a/2}\left(\sum_{i=0}^{1} g_u^i(T)\,\frac{\partial^i \hat{z}_u}{\partial T^i}(T) + \sum_{i=0}^{1} g_v^i(T)\,\frac{\partial^i \hat{z}_v}{\partial T^i}(T) + \sum_{i=0}^{2} g_w^i(T)\,\frac{\partial^i \hat{z}_w}{\partial T^i}(T)\right)\mathrm{d}T = 0 \tag{78}$$

for any set of test functions $(\hat{z}_u, \hat{z}_v, \hat{z}_w)$, where the coefficients are given by

$$\begin{array}{rcl} g_u^0(T) &=& -f_T \\ g_u^1(T) &=& K\,(\partial_T z_u + \partial_T Y_w^{\boldsymbol{h}}\,\partial_T z_w + \nu\,\boldsymbol{h}^\dagger \cdot \nabla Y_v^{\boldsymbol{h}}) \\ g_v^0(T) &=& -(f_S + \boldsymbol{h}^\dagger \cdot \nabla n_{SS}^{[0]\star}) \\ g_v^1(T) &=& \dfrac{K\,(1-\nu)}{2}\left(\partial_T z_v + \kappa_3\,(z_w - T\partial_T z_w) + \boldsymbol{h}^\dagger \cdot \nabla Y_u^{\boldsymbol{h}}\right) \\ g_w^0(T) &=& \kappa_3\,g_v^1(T) - f_\mathrm{n} - f_\mathrm{t}\,T + T(\kappa_3^\dagger\,n_{SS}^{[0]\star} + \kappa_3\,\boldsymbol{h}^\dagger \cdot \nabla n_{SS}^{[0]\star}) \\ g_w^1(T) &=& -\kappa_3\,T g_v^1(T) + \partial_T Y_w^{\boldsymbol{h}}\,g_u^1(T) - 2\,\boldsymbol{h}^\dagger \cdot \nabla m_{ST}^{[0]\star} \\ g_w^2(T) &=& D(\partial_{TT} z_w - \nu T \kappa_3^\dagger) \end{array} \tag{79}$$

The solution z_u, z_v and z_w are found with the help of a symbolic calculation language in the form 8th, 8th, and 7th degree polynomials in T, respectively. Inserting these polynomials in the expressions in Subsection 5.3, we obtain the second order strain energy term as

$$\frac{1}{2}\boldsymbol{\hbar}'(S)\cdot\boldsymbol{B}(\boldsymbol{\hbar}(S))\cdot\boldsymbol{\hbar}'(S)) = \frac{1}{2}\left[-\frac{Ya^5 t\,\nu}{180}\kappa_3(S)\,\varepsilon'(S)\,\kappa_3'(S) + \frac{Ya^3\,t^3}{5040\,(1-\nu^2)}\kappa_3'^2(S)\,\eta_1\!\left(\frac{\kappa_3(S)}{\kappa^\star}, \frac{c}{\kappa^\star}, \nu\right)\right], \tag{80}$$

where $\kappa^\star$ is the typical strain defined in (49) and

$$\eta_1(\bar{\kappa}_3, \bar{c}, \nu) = (1-\nu)\,(27 + 71\,\nu) - \frac{1}{360}\left(\frac{1}{2640}\,\bar{\kappa}_3^4 + (38 + 75\,\nu)\,\bar{\kappa}_3^2\right) + \frac{23}{144}\,\bar{c}^2.$$

The boundary terms is obtained similarly, the result being

$$\boldsymbol{C}(\boldsymbol{\hbar}(S))\cdot\boldsymbol{\hbar}'(S) \;=\; \frac{1}{2}\frac{Ya^5\,t\,\nu}{360}\kappa_3^2(S)\,\varepsilon'(S) + \frac{1}{2}\frac{Ya^3\,t^3}{1260\,(1+\nu)}\kappa_3(S)\,\kappa_3'(S)\,\eta_2\!\left(\frac{\kappa_3(S)}{\kappa^\star}, \nu\right) \tag{81}$$

where

$$\eta_2(\bar{\kappa}_3, \nu) = 4 - 11\,\nu + \frac{1}{950400}\,\frac{1}{(1-\nu)}\,\bar{\kappa}_3^4 + \frac{1}{1440}\,\frac{(34 + 67\,\nu)}{(1-\nu)}\,\bar{\kappa}_3^2.$$

Bibliography

[1] K. A. Seffen and S. Pellegrino. Deployment dynamics of tape springs. *Proceedings of the Royal Society of London. Series A: Mathematical, Physical and Engineering Sciences*, 455(1983):1003–1048, 1999.

[2] K. A. Seffen, Z. You, and S. Pellegrino. Folding and deployment of curved tape springs. *International Journal of Mechanical Sciences*, 42(10):2055–2073, 2000.

[3] J. Black, J. Whetzal, B. deBlonk, and J. Massarello. Deployment repeatability testing of composite tape springs for space optics applications. In *47th AIAA/ASME/ASCE/AHS/ASC Structures, Structural Dynamics, and Materials Conference 14th AIAA/ASME/AHS Adaptive Structures Conference 7th*, page 1905. 2006.

[4] T. Murphey, G. E. Sanford, and S. Jeon. Deployable space boom using bi-stable tape spring mechanism. July 2014. US Patent 8,770,522.

[5] M. Bergou, M. Wardetzky, S. Robinson, B. Audoly, and E. Grinspun. Discrete elastic rods. In *ACM SIGGRAPH 2008 papers*, pages 1–12. 2008.

[6] C. Lestringant, B. Audoly, and D. M. Kochmann. A discrete, geometrically exact method for simulating nonlinear, elastic or non-elastic beams. *Computer Methods in Applied Mechanics and Engineering*, 361:112741, 2020.

[7] E. Doedel, A. R. Champneys, F. Dercole, T. F. Fairgrieve, Y. A. Kuznetsov, B. Oldeman, R. C. Paffenroth, B. Sandstede, X. J. Wang, and C. H. Zhang. Auto-07p: continuation and bifurcation software for ordinary differential equations. 2007.

[8] W. Wuest. Einige Anwendungen der Theorie der Zylinderschale. *ZAMM-Journal of Applied Mathematics and Mechanics/Zeitschrift für Angewandte Mathematik und Mechanik*, 34(12):444–454, 1954.

[9] E. H. Mansfield. Large-deflexion torsion and flexure of initially curved strips. *Proceedings of the Royal Society of London. A. Mathematical and Physical Sciences*, 334(1598):279–298, 1973.

[10] J. Carr, M. E. Gurtin, and M. Slemrod. Structured phase transitions on a finite interval. Technical Report, Carnegie-Mellon institute of research, Pittsburgh (PA), USA, 1984.

[11] M. Martin, S. Bourgeois, B. Cochelin, and F. Guinot. Planar folding of shallow tape springs: the rod model with flexible cross-section revisited as a regularized Ericksen bar model. *International Journal of Solids and Structures*, 188:189–209, 2020.

[12] F. Guinot, S. Bourgeois, B. Cochelin, and L. Blanchard. A planar rod model with flexible thin-walled cross-sections. application to the folding of tape springs. *International Journal of Solids and Structures*, 49(1):73–86, 2012.

[13] E. Picault, P. Marone-Hitz, S. Bourgeois, B. Cochelin, and F. Guinot. A planar rod model with flexible cross-section for the folding and the dynamic deployment of tape springs: improvements and comparisons with experiments. *International Journal of Solids and Structures*, 51(18):3226–3238, 2014.

[14] E. Picault, S. Bourgeois, B. Cochelin, and F. Guinot. A rod model with thin-walled flexible cross-section: extension to 3d motions and application to 3d foldings of tape springs. *International Journal of Solids and Structures*, 84:64–81, 2016.

[15] E. Carrera, A. Pagani, and A. G. de Miguel. Nonlinear analysis of composite tape springs by refined beam models. In *Proceedings of the AIAA SciTech Forum 2020*. 2020.

[16] Z. Soltani and M. Santer. Efficient geometrically-nonlinear analysis of tape spring flexures using a unified beam formulation. In *Proceedings of the AIAA Scitech 2021 Forum 11–21 January 2021*. 2021.

[17] C. Lestringant and B. Audoly. Asymptotically exact strain-gradient models for nonlinear slender elastic structures: a systematic derivation method. *Journal of the Mechanics and Physics of Solids*, 136:103730, 2020.

[18] C. Lestringant and B. Audoly. A diffuse interface model for the analysis of propagating bulges in cylindrical balloons. *Proceedings of the Royal Society A: Mathematical, Physical and Engineering Sciences*, 474(2218):20180333, 2018.

[19] C. Lestringant and B. Audoly. A one-dimensional model for elasto-capillary necking. *Proceedings of the Royal Society A*, 476(2240):20200337, 2020.

[20] B. Audoly and S. Neukirch. A one-dimensional model for elastic ribbons: a little stretching makes a big difference. *Journal of the Mechanics and Physics of Solids*, 153:104457, 2021.

[21] B. Audoly and C. Lestringant. Asymptotic derivation of high-order rod models from non-linear 3d elasticity. *Journal of the Mechanics and Physics of Solids*, 148:104264, 2021.

[22] D. H. Hodges. *Nonlinear composite beam theory*. American Institute of Aeronautics and Astronautics, 2006.

[23] J. Langer and D. A. Singer. Lagrangian aspects of the Kirchhoff elastic rod. *SIAM Review*, 38(4):605–618, 1996.

[24] B. Durand, A. Lebée, P. Seppecher, and K. Sab. Predictive strain-gradient homogenization of a pantographic material with compliant junctions. *Journal of the Mechanics and Physics of Solids*, 160:104773, jan 2022.